SPACE RESEARCH IN SLOVAKIA

2010 - 2011

SLOVAK ACADEMY OF SCIENCES

COSPAR

SLOVAK NATIONAL COMMITTEE

MARCH 2012

ISBN 978-80-970779-5-2
EAN 9788097077952

Contents.

1. EXPERIMENTS FOR MEASUREMENTS IN SPACE

1.1 Experiment MEP-2 for project RADIOASTRON

The experiment MEP-2 was successfully launched on board of Spectrum - RADIOASTRON satellite on 18 July 2011 from Baikonur cosmodrome. The satellite Radioastron was injected to excentric orbit with initial apogee 390000 km, perigee 10000 km and inclination 51,6 deg. The programmable spectrometer of energetic particles MEP-2 was developed and constructed at the Department of Space Physics of Institute of Experimental Physics, Slovak Academy of Science, Košice (IEP SAS) in cooperation with Space Research Institute of Russian Academy of Sciences (IKI-RAN) and Democritus University of Thrace, Greece. The spectrometer is a part of the Plasma-F science suite conducted by IKI-RAN (http://www.plasma-f.cosmos.ru/en/instruments). MEP-2 operates in space nominally, however, during unfavourable spacecraft orientation, some parts of registered data are contaminated by the sunlight.

Fig. 1. Programmable particle spectrometer MEP-2 (Flight Model).

Fig. 2. MEP-2 installed on board of Spectrum-Radioastron satellite.

Fig. 3. Successful launch of ZENIT-E rocket with Radioastron on board from Baikonur cosmodrome.

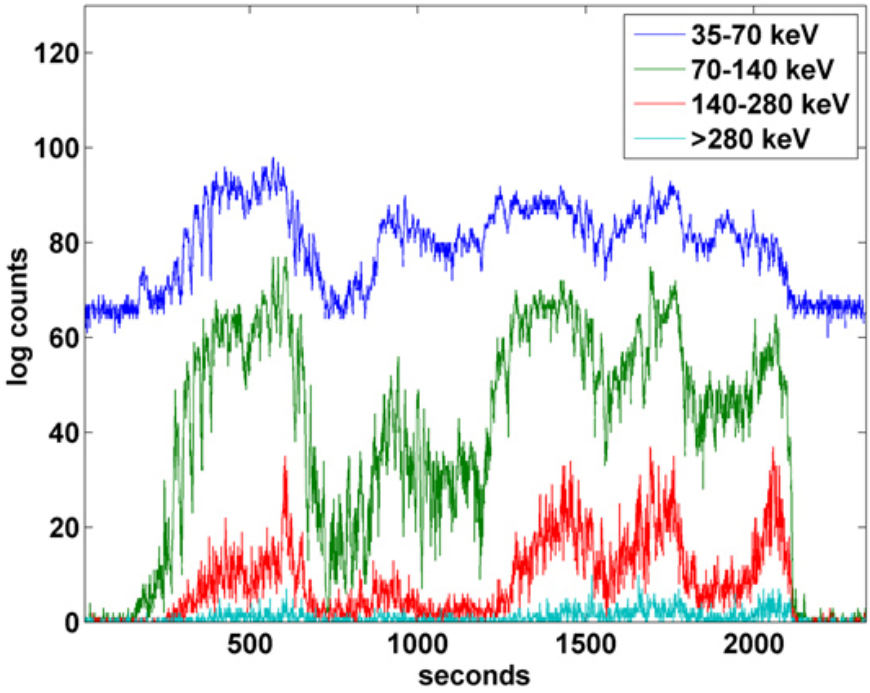

Fig. 4. First MEP-2 data from the orbit (four energy channels of the 1P ion detector).

1.2 Experiment DOK-M for project RESONANCE

The experiment DOK-M is presently under development at IEP SAS in cooperation with IKI-RAN and Democritus University of Thrace, Greece for project RESONANCE.

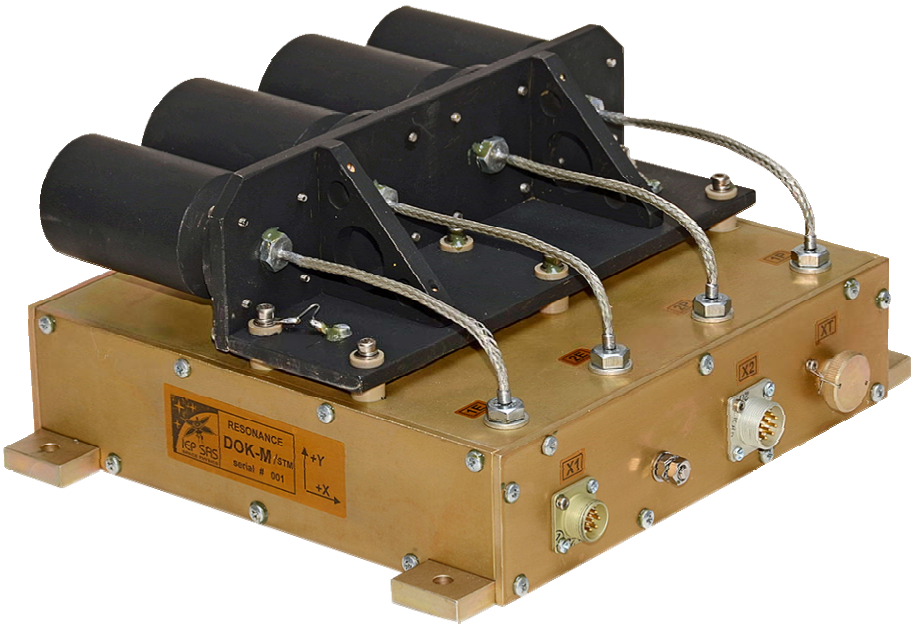

Fig. 5. Particle spectrometer DOK-M /STM (Structural Thermal Model).

The project RESONANCE is a magnetospheric space exploration mission conducted by IKI-RAN and dedicated for advanced study of the wave – particle interactions in the Earth's magnetosphere (http://www.iki.rssi.ru/resonance). Earth's magnetosphere, as natural resonator for many types of electromagnetic waves, is a place where electromagnetic waves efficiently interact with charged energetic particles via cyclotron resonance.

The mission consists of four spacecraft in specific Earth orbits, within the same magnetic flux tube for a certain period of time.

Two models of the DOK-M spectrometer will be installed on board of two satellites of the RESONANCE project. The launch is scheduled for 2015.

1.3 Experiment ASPECT-L for project Luna Glob

The experiment ASPECT-L is presently under development at IEP SAS in cooperation with IKI-RAN and Democritus University of Thrace, Greece for Moon exploration mission Luna Glob.

The mission includes Orbiter module and Lander module.

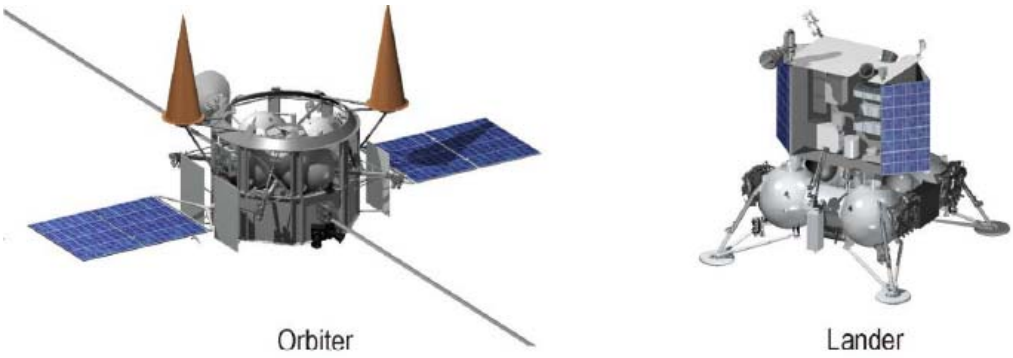

Fig. 6. Orbiter and Lander of the Luna Glob mission.

The ASPECT-L energetic particle spectrometer will be installed on the Orbiter module.

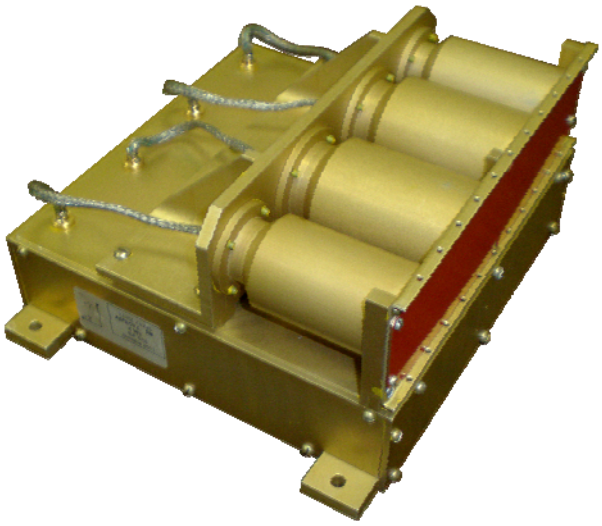

Fig. 7. Energetic particle spectrometer ASPECT-L (Structural Thermal Model).

1.4 Experiment PICAM for mission ESA-BepiColombo

In the frame of collaboration with Space Technology Ireland (STIL) and Austrian Space Research Institute (IWF), Department of Space Physics IEP-SAS contributes to development and manufacture of the electronic box of the planetary ion camera PICAM for ESA mission BepiColombo to planet Mercury.

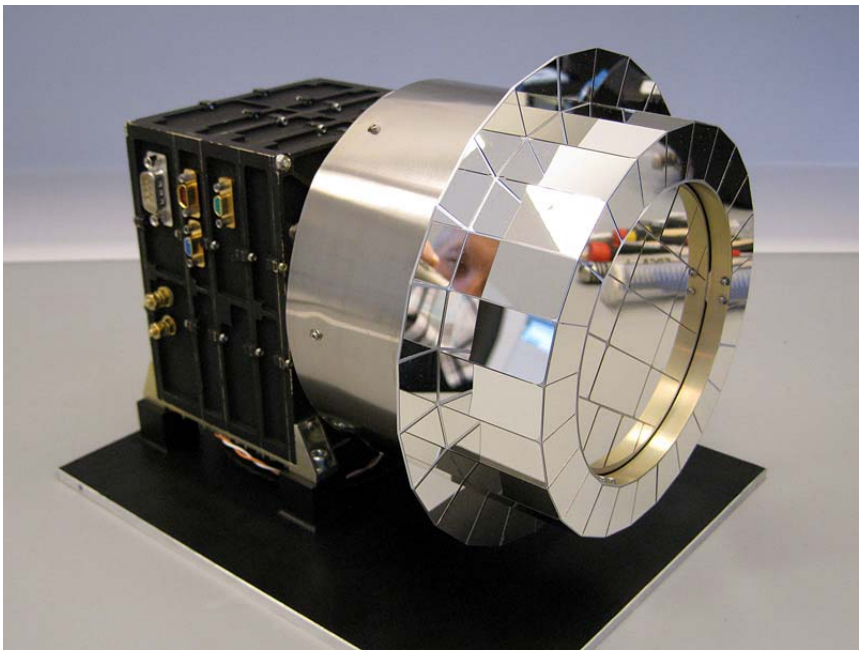

Fig. 8. Planetary ion camera PICAM (Structural Thermal Model).

1.5. Participation of Slovakia in the project JEM-EUSO.

JEM-EUSO (Japanese Experiment Module - Extreme Universe Space Observatory) experiment will search for UHECR (energy above 10^{19} eV) by monitoring UV light produced in their interaction with atmosphere from International Space Station (http://jemeuso.riken.jp/en/index.html).

Department of Space Physics IEP-SAS estimated an operational duty cycle for JEM-EUSO experiment along the ISS trajectory. Two main approaches are used. First by the analytical evaluation of possible UV light sources on the Earth nightside where main sources are UV moon light and UV background intensities created by nightglow, stars and effect of artificial sources in populated areas. In the second approach we have used the Universitetsky Tatiana satellite data from the measurements in the period from 2005 till 2007.

UHECR events are very rare and JEM-EUSO experiment will measure during his 3 years or longer stay at International Space Station very big amount of data. Department of Space Physics IEP-SAS provides an analysis of the fake trigger events obtained by JEM-EUSO simulation code to estimate a how many fake (i.e not real) events can JEM-EUSO detector see.

Fig. 9. JEM-EUSO onboard ISS.

IEP SAS contributed to the estimation of the time fraction on the orbit of ISS where the JEM-EUSO measurements will be not affected by the other

processes (not due to the cosmic ray interactions) in the atmosphere producing the ultraviolet emissions observed above the atmosphere. For that the available data from Russian satellite Universitetsky Tatyana have been used.

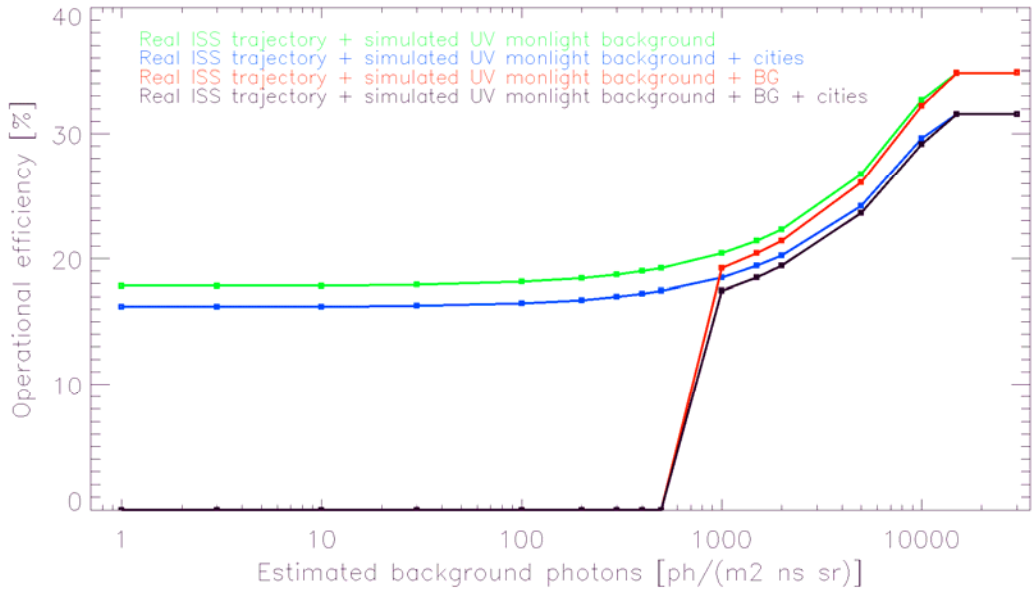

Fig. 10. Operational duty cycle evaluated along real ISS trajectory in years 2005 till 2007 with simulated moonlight (green line), moonlight together with oceanequivalent UV background (red), moonlight together with oceanequivalent UV background (blue) and all sources i.e. moon, oceanequivalent background and cities together (black).

2. SPACE PHYSICS, GEOPHYSICS AND ASTRONOMY

Activities of institutions in Slovakia related to the space solar physics and X-ray astronomy, interplanetary matter and explorations of the comets, solar wind and its interactions with the Earth's magnetosphere, energetic particles in the magnetosphere and in interplanetary space, atmosphere and ionosphere of the Earth, are continuing in various institutes in Slovakia. The following short survey presents selected activities of the abovementioned directions and the obtained results.

The ***Institute of Experimental Physics, SAS, Košice*** (IEP SAS, its Department of Space Physics, http://space.saske.sk) in collaboration with the laboratories in abroad continued studies of the dynamics of cosmic rays and of cosmic particles with the energies well below those of cosmic rays and well above those of solar wind (from few tens of keV up to several MeV). In The methodological works were conducted jointly with the team of magnetic field measurements on Venus-Express. The analysis of the data obtained both from the low altitude and high apogee satellites, as well as development and construction of new instruments for the future studies continued in the period 2008-2009. In addition, new results have been obtained from the measurements of ground based neutron monitors, one of them at Lomnicky stit (http://neutronmonitor.ta3.sk).

The MEP-2 data (data processing by M. Slivka) were registered by SSNI telemetry and after their transmissions to the Earth they are processed at IEP SAS Košice. MEP-2 was switched on 30 July 2011 in the solar wind, and since then is operating almost permanently with the exception of the near perigee zones within approximately 10 R_E from Earth, where the instrument is switch-off in order to avoid saturation due to high particle flux in the inner magnetosphere. During this period we processed more then 200 files with measurement of electrons and protons fluxes and spectra.

Fig. 1 shows temporal profiles of the integral fluxes of protons as observed by the detectors P1 and P2 during a short period on August 22, 2011 in the position well outside the bow shock. MEP-2 operated in the mode 22, which enabled to observe electron and ion flux in 32 energy channels. The two increases around 0645 and 0653 UT correspond most probably to the time of connection of the spacecraft along the field line to the bow shock. The electrons did not show any significant increase during these periods.

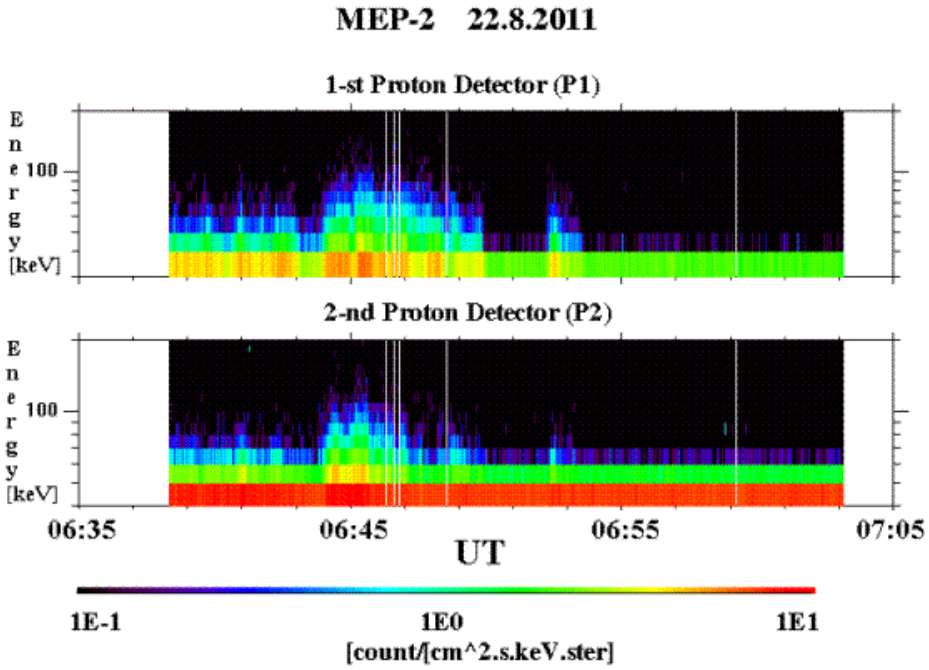

Fig. 1. The energy spectrogram of the proton detectors measured by MEP-2 during August 22, 2011. The sum of two neighbour energy channels is plotted (16 energy intervals).

The measurements of MEP-2 instrument are realized in the period of increasing solar activity. Figure 2 shows the pulsating flux of protons with energy up to at least 100 keV in the region upstream of the bow shock.

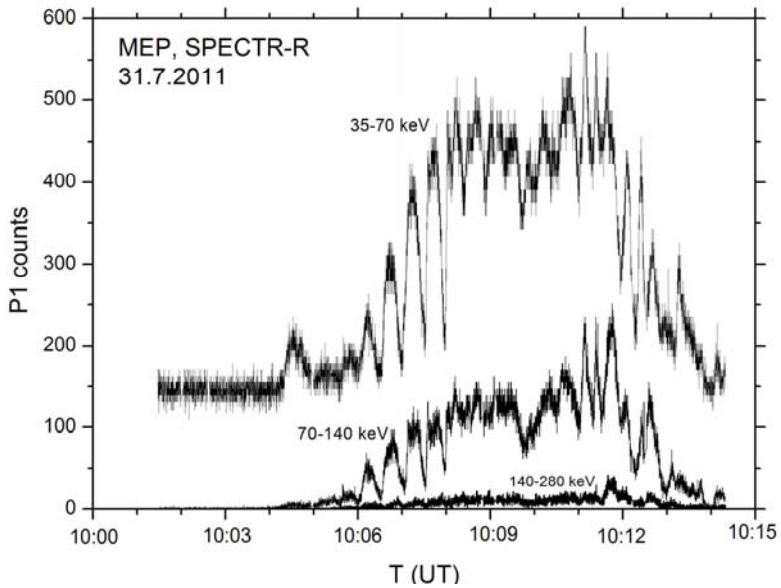

Fig.2. Pulsations with period ~ 30 s in the proton flux observed in the region upstream from the bow shock by MEP-2.

Measurements by MEP-2 on SPEKTR-R can be utilized for multisatellite energetic particle studies e.g. in comparison with the data by ACE, SOHO, GEOTAIL and THEMIS in the future.

Data from CORONAS-F satellite have been used to check how the geomagnetic field model with external currents can explain the penetration of several MeV solar protons deep into the inner magnetosphere (Lazutin et al., 2011). Chapter by (Kudela and Lazutin, 2011) surveys the potential possibilities of low altitude polar orbiting satellites with large geometric factors for high energy particles (e.g. CORONAS-F) for (a) estimates of energy spectra of solar or interplanetary accelerated particles by checking the outer zone boundary of trapping and for (b) checking how the different geomagnetic field models are fitting the observed trapped particle profiles in different local time sectors.

Independently on the state of magnetosphere, the measurements of energetic "neutral emissions" (gammas and neutrons) near the Earth or on the ground, serve as indicator of acceleration processes on solar surface. Papers (Kurt et al., 2010a; 2010b; Kuznetsov et al., 2011) analyze the high energy gamma ray emissions and neutrons observed during the solar flares by SONG instrument on CORONAS-F satellite as well as dynamics of protons related to solar flares. Figure 3 is indicating the change of energy spectra of gamma rays during one of the flares with gamma rays. Clear onset time of π^o production due to interactions of protons accelerated in the solar flare and consecutive decay into two gamma quanta.

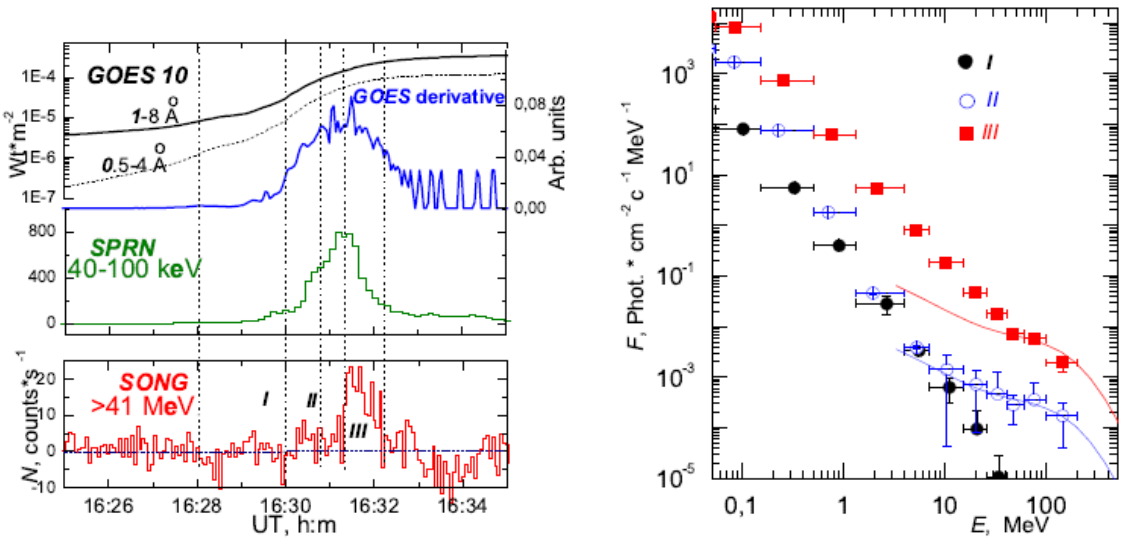

Fig. 3. Profile of photon flux of various energies and energy spectra during three time intervals around the time of solar flare on August 25, 2001.

McKenna et al (2010) and Li et al (2010) using the data from NUADU experiment on satellite Double Star and data from other satellites analyzed the reconfiguration of the magnetosphere by energetic neutral atom images during the geomagnetic storms in January 2005 and in May 2005.

Firoz et al (2010; 2011a; 2011b) discuss the possible mechanisms of the GLEs and relations to CMEs. Quasi-periodic variations of cosmic rays observed by neutron monitors including that on Lomnicky stit and using the neutron monitor database constructed and updated at http://nmdb.eu have been analyzed in papers (Kudela et al, 2010; Mavromichalaki et al, 2011; Sabbah and Kudela, 2011). Modulation of antiprotons and estimates of proton to antiproton flux to be measured in new experiment AMS-2 has been obtained by the simulation technique of cosmic ray propagation in the heliosphere (Bobík et al, 2011).

Jansen et al. (2011) reviewed the current status from the scientific and technological point of view of solar energetic particles, solar and galactic cosmic ray measurements as well as high energy UV-, X- and gamma-ray imaging of the Sun, and proposes a novel space application due to their counting and imaging capabilities. Papailiou et al. (2011a,b) indicate that geomagnetic changes as well as changes of cosmic ray intensity are connected to variations of the human physiological parameters, as studied in the sample of health state of aviators investigated in the Air Force Hospital in Kosice, Slovakia, over long time period.

Paper by Pope et al. (2011) describes the methodological works important for the cleaning of magnetic field measurement on Venus Express (MAG-VEX experiment, PI T.L. Zhang, Austria) done with participation of IEP SAS.

References:

1. BOBÍK, P. - BOSCHINI, J. M. - CONSOLANDI, C. - DELLA TORRE, S. - GERVASI, M. - GRANDI, D. - KUDELA, K. - PENSOTTI, S. - RANCOITA, G. P. (2011). Antiproton modulation in the Heliosphere and AMS-02 antiproton over proton ratio prediction, Astrophys. Space Sci. Trans., 7, 1–5.

2. FIROZ, K. A. - CHO, K. S. - HWANG, J. - KUMAR, D. V. - PHANI LEE, J. J. - OH, S. Y. - KAUSHIK, SUBHASH C. - KUDELA, K. - RYBANSKÝ, M. - DORMAN, - LEV I. (2010). Characteristics of ground-level enhancement-

associated solar flares, coronal mass ejections, and solar energetic particles, J. Geophys. Res., Space Phys., 115, Art. No. A09105, DOI 10.1029/2009JA015023, Sep. 14.

3. FIROZ, K. A. - MOON, Y. J. - CHO, K. S. - HWANG, J. - PARK, Y. D. - KUDELA, K. - DORMAN, L. I. (2011a). On the relationship between ground level enhancement and solar flare. J. Geophys. Res., Space Phys., 116, Art. No. A04101, DOI 10.1029/2010JA016171, Apr. 1.

4. FIROZ, K. A. - MOON, Y. J. - PARK, S. H. - KUDELA, K. - ISLAM, J. N. - DORMAN, L. I. (2011b). On the possible mechanisms of two ground-level enhancement events, Astrophys. J., 743, Is 2, Art 190, DOI 10.1088/0004-637X/743/2/190, Dec. 20.

5. JANSEN, F. - BEHRENS, J. - POSPÍŠIL, S. - KUDELA, K. (2011). Space situational awareness satellites and ground based radiation counting and imaging detector technology, Nucl. Instrum. Meth. In Phys. Res. Section A, vol. 633, S231-S234, DOI 10.1016/j.nima.2010.06.175, May.

6. KUDELA, K. - LAZUTIN, L. L. (2011). Selected Solar Influences on the Magnetosphere: Information from Cosmic Rays. In Sun, the solar wind and the heliosphere, Editors Mari Paz Miralles, Jorge Sanchez Almeida. IAGA Special Sopron Book Series, vol. 4, 199-207, DOI 10.1007/978-90-481-9787-3_18, Springer.

7. KUDELA, K. - MAVROMICHALAKI, H. - PAPAIOANNOU, A. - GERONTIDOU, M. (2010). On Mid-Term Periodicities in Cosmic Rays, Sol. Phys., 266, 1, 173-180, DOI 0.1007/s11207-010-9598-0, Sep.

8. KURT, V. G. - SVERTILOV, S. I. - YUSHKOV, B. YU. - BOGOMOLOV, A. V. - GRECHNEV, V. V. - GALKIN, V. I. - BOGOMOLOV, V. V. - KUDELA, K. - LOGACHEV, YU. I. - MOROZOV, O. V. - MYAGKOVA, I. N. (2010a). Dynamics and energetics of the thermal and nonthermal components in the solar flare of January 20, 2005, based on data from hard electromagnetic radiation detectors onboard the CORONAS-F satellite, Astron. Lett., 36, 4, 280-291, DOI 10.1134/S1063773710040067, Apr.

9. KURT, V. G. - YUSHKOV, B. YU. - KUDELA, K. - GALKIN, V. I. (2010b). High-energy gamma radiation of solar flares as an indicator of acceleration of energetic protons, Cosmic Res., 48, 1, 70-79, DOI 10.1134/S0010952510010053, Feb.

10. KUZNETSOV, S. N. - KURT, V. G. - YUSHKOV, B. YU. - KUDELA, K. - GALKIN, V. I. (2011). Gamma-Ray and High-Energy-Neutron Measurements on CORONAS-F during the Solar Flare of 28 October 2003, Sol. Phys., 268, 1, 175-193, DOI 10.1007/s11207-010-9669-2, Jan.

11. LAZUTIN, L. L. - GOTSELYUK, YU. V. - MURAV'EVA, E. A. - MYAGKOVA, I. N. - PANASYUK, M. I. - STAROSTIN, L. I. - YUSHKOV, B. YU. - KUDELA, K. - HASEBE, N. - SUKURAI, K. - HAREYAMA, M. (2010). Dynamics of solar protons in the Earth's magnetosphere during magnetic storms in November 2004-January 2005, Geomagn. Aeron., 50, 2, 168-180, DOI 10.1134/S0016793210020040, Apr.

12. LAZUTIN, L. L. - MURAV'EVA, E. A. - KUDELA, K. - SLIVKA, M. (2011). Verification of magnetic field models based on measurements of solar cosmic ray protons in the magnetosphere, Geomagn. Aeron. 51, 2, 198-209, DOI 10.1134/S0016793211010087, Apr.

13. LI, LU - MCKENNA-LAWLOR, S. - BARABASH, S. - BRANDT, P. C. - BALÁŽ, J. - LIU, Z. X. - HE, Z. H. - REEVES, G. D. (2010). Comparisons between ion distributions retrieved from ENA images of the ring current and contemporaneous, multipoint ion measurements recorded in situ during the major magnetic storm of 15 May 2005, J. Geophys. Res., Space Phys., 115, Art. No. A12218, DOI 10.1029/2010JA015770, Dec. 8.

14. MAVROMICHALAKI, H. - PAPAIOANNOU, A. - PLAINAKI, C. - SARLANIS, C. - SOUVATZOGLOU, G. - GERONTIDOU, M. - PAPAILIOU, M. - EROSHENKO, E. - BELOV, A. - YANKE, V. - FLUEKIGER, E. O. - BUETIKOFER, R. - PARISI, M. - STORINI, M. - KLEIN, K. L. - FULLER, N. - STEIGIES, C. T. - ROTHER, O. M. - HEBER, B. - WIMMER-SCHWEINGRUBER, R. F. - KUDELA, K. - STRHARSKY, I. - LANGER, R. - USOSKIN, I. - IBRAGIMOV, A. - CHILINGARYAN, A. - HOVSEPYAN, G. - REYMERS, A. - YEGHIKYAN, A. - KRYAKUNOVA, O. - DRYN, E. - NIKOLAYEVSKIY, N. - DORMAN, L. - PUSTIL'NIK, L. (2011). Applications

and usage of the real-time Neutron Monitor Database, Adv. Space Res., vol. 47, Is. 12, 2210-2222, DOI 10.1016/j.asr.2010.02.019, Jun 15.

15. MCKENNA-LAWLOR, S. - LI, LU - DANDOURAS, I. - BRANDT, P. C. - ZHENG, Y. - BARABASH, S. - BUČÍK, R. - KUDELA, K. - BALÁŽ, J. - STRHÁRSKÝ, I. (2010). Moderate geomagnetic storm (21-22 January 2005) triggered by an outstanding coronal mass ejection viewed via energetic neutral atoms, J. Geophys. Res., Space Phys., 115, Art. No. A08213, DOI 10.1029/2009JA014663, Aug. 14.

16. PAPAILIOU, M. - MAVROMICHALAKI, H. - KUDELA, K. - ŠTETIAROVÁ, J. - DIMITROVA, S. (2011a). Effect of geomagnetic disturbances on physiological parameters: An investigation on aviators, Adv. Space Res., vol. 48, Is. 9, 1545-1550, DOI 10.1016/j.asr.2011.07.004, Nov. 1.

17. PAPAILIOU, M. - MAVROMICHALAKI, H. - KUDELA, K. - ŠTETIAROVÁ, J. - DIMITROVA, S. - GIANNAROPOULOU, E. (2011b). The effect of cosmic ray intensity variations and geomagnetic disturbances on the physiological state of aviators, Astrophys. Space Sci. Trans., 7, 373-377.

18. POPE, S. A. - ZHANG, T. L. - BALIKHIN, M. A. - DELVA, M. - HVIZDOŠ, L. - KUDELA, K. - DIMMOCK, A. P. (2011). Exploring planetary magnetic environments using magnetically unclean spacecraft: a systems approach to VEX MAG data analysis, Ann. Geophys., 29, 4, 639 – 647, DOI 10.5194/angeo-29-639-2011.

19. SABBAH, I. - KUDELA, K. (2011). Third harmonic of the 27 day periodicity of galactic cosmic rays: Coupling with interplanetary parameters, J. Geophys. Res., Space Phys., vol. 116, Art A04103, DOI 10.1029/2010JA015922, Apr. 2.

Last 2 years the activities of the ***Faculty of Mathematics, Physics and Informatics, Comenius University, Bratislava***, have been oriented mainly in the study of cosmic rays and their interaction with material objects.

In (2) measurements of cosmogenic nuclides in up to 11 bulk samples from various depths in Norton County are reported. The activities of ^{36}Cl, ^{41}Ca, ^{26}Al, and ^{10}Be were measured by accelerator mass spectrometry; the concentrations of the stable isotopes of He, Ne, Ar, and Sm were measured by electron and thermal ionization mass spectrometry, respectively. Production rates for the nuclides were modeled using the LAHET and the Monte Carlo N-Particle codes. Assuming a one-stage irradiation of a meteoroid with a pre-atmospheric radius of approximately 50 cm, the model satisfactorily reproduces the depth profiles of ^{10}Be, ^{26}Al, and ^{53}Mn (<6%) but overestimates the ^{41}Ca concentrations by about 20%. ^{3}He, ^{21}Ne, and ^{26}Al data give a one-stage cosmic-ray exposure (CRE) age of 115 Ma. Argon-36 released at intermediate temperatures, $^{36}Ar_n$, is attributed to production by thermal neutrons. From the values of $^{36}Ar_n$, an assumed average Cl concentration of 4 ppm, and a CRE age of 115 Ma, we estimate thermal neutron fluences of 1–4 × 10^{16} neutrons cm^{-2}. We infer comparable values from $\varepsilon^{149}Sm$ and $\varepsilon^{150}Sm$. Values calculated from ^{41}Ca and a CRE age of 115 Ma, 0.2–1.4 × 10^{16} neutrons cm^{-2}, are lower by a factor of approximately 2.5, indicating that nearly half of the ^{149}Sm captures occurred earlier. One possible irradiation history places the center of proto-Norton County at a depth of 88 cm in a large body for 140 Ma prior to its liberation as a meteoroid with a radius of 50 cm and further CRE for 100 Ma.

A comprising thermodynamic approach is presented in (3) to investigate the behavior of saline solutions with respect to $CaCO_3$, $CaSO_4$ and SiO_2 scaling in water treatment processes. Thr Pitzer activity coefficient model is used to describe the aqueous species activities and the corresponding equilibrium reactions are solved to determine the saline solution composition. A well evaluated parameter set for the system H-Na-Ca-Mg-OH-Cl-CO_3-HCO_3-CO_2-SO_4-HSO_4-SiO_2 at 25°C is compiled and applied for calculation of the pure scale solubilities as well as mixture effects such as $CaCO_3$/$CaSO_4$ coprecipitation and silica adsorption. New data on silica removal dependant on the saline solution composition are used to estimate the ratio of silicate formation and silica adsorption onto other precipitating salts. Whereas the saturation states for pure scales are found to be well predictable at varying conditions, only qualtitative estimations for mixed scale formation can be

achieved. Here, the predictability by thermodynamic equilibrium calculation is shown to meet its present boundary and its valuable service for understanding the mechanisms of scaling and the species involved is highlighted.

In (4) the cosmogenic radionuclides ^{10}Be, ^{26}Al and ^{53}Mn and stable He-, Ne- and Ar-isotopes were measured in differentiated meteorites from Antarctica using accelerator mass spectrometry, γ-γ-coincidence techniques, radiochemical neutron activation analysis and conventional mass spectrometry. No depth effects were seen in meteorites from which several samples were analyzed. In most of the meteorites ^{10}Be and ^{26}Al were in saturation at time of fall, but the ^{26}Al concentrations are partially lowered by substantial terrestrial ages. For ^{10}Be some extremely low concentrations were found which cannot be explained by the decay during terrestrial residence. The experimental data are discussed together with rare gas measurements in the context of model calculations of the depth- and size-dependent production of cosmogenic nuclides in differentiated stony meteorites. Based on the model calculations minimal exposure ages, and shielding corrected ^{21}Ne exposure ages were calculated. A detailed discussion of the production rates and of possible pairing of meteorites is given.

A model is presented in (5) which permits the calculation of production rates of cosmic-ray-produced light noble gases He, Ne and Ar as well as ^{10}Be, ^{26}Al and ^{53}Mn in chondrites of variable size and shape The production of a given nuclide is described by a semi-empirical equation used by SIGNER and NIER (1960) to describe the production of the light noble gases in the iron meteorite Grant. For a given nuclide, this equation contains two free parameters that are fitted to the depth profiles measured in the Knyahinya chondrite. Model predictions are tested by comparison with literature data for depth profiles in other meteorites (ALH78084, St. Severin, Keyes). The agreement between model predictions and experimental data is found to be 5̃% for the concentrations of ^{10}Be, ^{21}Ne, ^{22}Ne, ^{38}Ar and ^{53}Mn, respectively and to be better than 1% for the ratios. The model predicts that 3-nuclide correlations that use the same reference nuclide are linear. The correlation between and ratios is experimentally verified over a wide range of irradiation conditions. With this relation, shielding and size corrected exposure ages can be derived from the measurements of ^{10}Be and of the Ne isotopes in a single sample. The calculated exposure ages are believed to have a precision of 5̃%.

References:

1. WELTEN, K. C. - CAFFEE, M. W. - HILLEGONDS, D. J. - McCOY, T. J. - MASARIK, J. - NISHIIZUMI, K. (2011). Cosmogenic radionuclides in L5 and LL5 chondrites from Queen Alexandra Range, Antarctica: Identification of a large L/LL5 chondrite shower with a preatmospheric mass of approximately 50,000 kg. Meteoritics & Planetary Science, 46, 177–196. doi: 10.1111/j.1945-5100.2010.01142.x

2. HERZOG, G. F. - ALBRECHT, A. - MA, P. - FINK, D. - KLEIN, J. - MIDDLETON, R. - BOGARD, D. D. - NYQUIST, L. E. - SHIH, C.-Y. - GARRISON, D. H. - REESE, Y. - MASARIK, J. - REEDY, R. C. - RUGEL, G. - FAESTERMANN, T. - KORSCHINEK, G., (2011). Cosmic-ray exposure history of the Norton County enstatite achondrite. Meteoritics & Planetary Science, 46, 284–310. doi: 10.1111/j.1945-5100.2010.01154.x

3. MERCHEL S. L. - BENEDETTI, D. L. - BOURLES, R. - BRAUCHER, A. - DEWALD, T. - FAESTERMANN, R. C. - FIKEL, G. - KORSCHINEK, J. - MASARIK, M. - POUTIVTSEV, P. - ROCHETTE, G. - RUGEL, K. O., ZELL, A. (2010). multi-radionuclide approach for in situ produced terrestrial cosmogenic nuclides: 10Be, 26Al, 36Cl and 41Ca from carbonate rocks, Nuclear Instruments and Methods in Physics Research Section B: Beam Interactions with Materials and Atoms, Volume 268, Issues 7–8, April 2010, Pages 1179-1184, ISSN 0168-583X, 10.1016/j.nimb.2009.10.128.

4. WELTEN, K. C. - CAFFEE, W. M. - HILLEGONDS, J. D. - MASARIK, J. - NISHIIZUMI, K. (2010). Identifying large chondrites using cosmogenic radionuclides, Nuclear Instruments and Methods in Physics Research Section B: Beam Interactions with Materials and Atoms, Volume 268, Issues 7–8, April 2010, Pages 1185-1188, ISSN 0168-583X, 10.1016/j.nimb.2009.10.129.

5. KIM, K. J. - MASARIK, J. - REEDY, R. C. (2010). Numerical simulations of production rates for 10Be, 26Al and 14C in extraterrestrial matter using the MCNPX code, Nuclear Instruments and Methods in Physics Research Section B: Beam Interactions with Materials and Atoms, Volume 268, Issues 7–8, April 2010, Pages 1291-1294, ISSN 0168-583X, 10.1016/j.nimb.2009.10.155.

In the ***Geophysical Institute of the Slovak Academy of Sciences, Bratislava and Hurbanovo***, a number of issues important within the frame of the space weather studies were investigated.

In [1] a model of the magnetic storm of August 4, 2010 has been studied. Here, the simulated Dst index series is obtained from an empirical model of the solar wind magnetosphere interaction and is compared with real data. A paraboloid 3D model of the magnetosphere has been used in order to compute magnetic fields in the region where the solar wind interacts with the Earth's magnetosphere. This part of the near Earth surroundings is known as the magnetopause and is usually of the main focus when modeling the interaction between the solar and planetary magnetic fields. The magnetic field exhibits a jump when moving from the solar wind (the external field) to the magnetosphere (the internal field). There is no normal component of the magnetic field at the magnetopause. As known from previous studies, the geomagnetic activity measured in terms of the Dst-index can be related with the jump in magnetic field.

In broader context, this can be concieved as a complementary approach to the space weather modelling, based on the first principles rather than statistics. The use of empirical models for the purposes of forecasting has the advantage of being less computationally demanding than global magnetohydrodynamic (MHD) models. Quantitative models should be able to replicate essential features of the response of the magnetospheric configuration to the variable external input. It is important to develop objective assessment criteria to determine which empirical models are most accurate, and where weaknesses in the models exist. Forecasting geomagnetic activity depends critically upon our ability to forecast the properties of the solar wind and its imbedded magnetic field, particularly the north-south component of the IMF when it encounters the magnetopause.

As a result of the study in [1] synthetic record of the geomagnetic storm has been obtained using empirical model. It is observable that considering longer past data record (in terms of backward hourly steps N) improves the model agreement with the storm return phase. From the point of view of prediction, it would be desirable to capture the onset of the disturbance as well. Adjusting scalings and parameters in empirical expressions can be the possible way towards improving the model response. At this point, it would be desirable

to benefit from combining the empirical study together with the use of the method of ANN; thereby setting up a more comprehensive model in a subsequent study.

Solar energetic particle (SEP) modelling has gained great interest in the community, specifically in connection with the safety of crews and the protection of technological systems of spacecraft situated outside the shielding of Earth's magnetosphere. Models for the prediction of SEP events have been studied in [2-7]. In [4] two models have been set up on the basis of a linear filter and on a special type of dynamic artificial neural network known as the layer-recurrent neural network. It appears to be correct that both CME and flare information are of great importance for the forecasting of large SEP events. Therefore it is appropriate to consider the following input parameters: the X-ray flare class for flares originating close to the centre of the solar disk; observed type II or IV radio bursts; and of the position angle, width, and linear speed of observed full or partial halo CMEs. The models are designed to provide forecasts of HEPFs (high energy proton fluxes) with energies exceeding 10 MeV at the L1 libration point.

In large SEP events it is apparent that the way in which SEPs are accelerated by a CME depends not only on the parameters of the CME in question. The preceding CMEs and/or flares that occurred in the same regions have to be taken into consideration as well. That is why special types of artificial neural networks, i.e. dynamic networks are believed to be helpful tools for SEP forecasting. as they can cope with temporal structures in studied time series. In other words, the prediction of SEP is performed, with focus on continuous time series rather than single solar SEP events. As for the single events approach, there can be difficulties to distinguish between the response of particular solar energetic particle events in case of their successive emergence. The response of interplanetary medium can be complicated by its `memory" effects, and therefore the forecast of SEP events should rely not only on current solar event data but should also consider the influence of past SEP data records.

The focus is made on the years 1998 – 2005. The reason is the frequency of CME occurrence. During these solar maximum years full or partial halo CMEs appeared frequently, approximately one event every 36 hours. Daily characteristics of CMEs, solar flares, and SEPs are used in the modelling. The characteristics of CMEs and flares are used as input parameters to the neural

network models. SEP characteristics are used as output parameters. The time series of observed as well as predicted SEP fluxes measured in terms of pfu (proton flux units) are shown in Fig.1.

From the practical point of view, the study in (4) is useful for providing tools for issuing alerts in case of increased HEPF. It is proposed to issue an alert for a succeeding 24-hour period if the model forecasts an overload of the critical HEPF level during that period, as well as when the overload was forecast for the previous 24-hour interval, and also if the overloaded HEPF was observed during the stated interval. If the critical level of HEPF was set to be 100 pfu, 28 SEP events were foreseen in time out of the 34 SEP total events occurring during the test period. It was carried off at the toll of 116 false alarms. In doing so, the rate of days when the safety measure was performed constituted 19% of all the tested days. The results obtained were still more encouraging when the critical level of HEPF was heightened to 200 pfu.

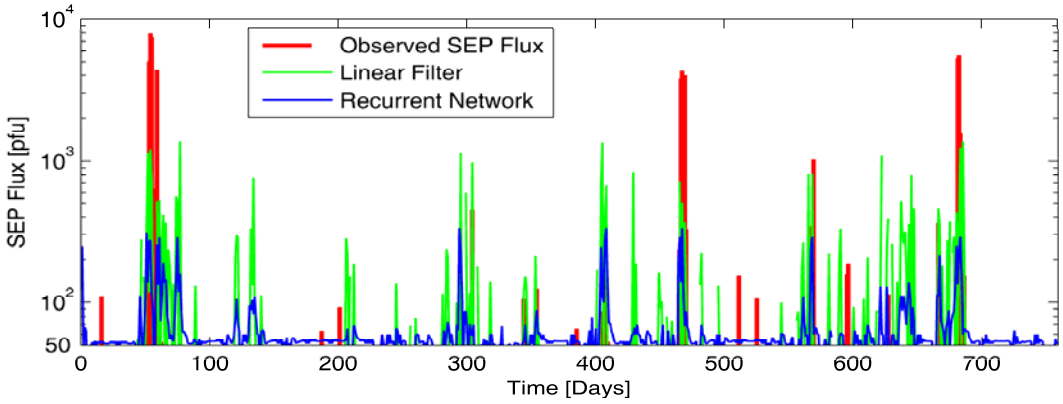

Fig. 1. Time series of SEP fluxes for the final test (13/08/2003 – 26/11/2005). Observed values are compared with those obtained as predictions of the linear filter (LF0) as well as with those modelled by the recurrent network (RNN).

Hurbanovo Geomagnetic Observatory of the GPISAS, is located at geographical latitude 47.87° and geographical longitude 18.18°. It performs continuous monitoring and registration of the geomagnetic field components. The one-minute mean values of all components of the geomagnetic field as well as the records acquired with the one-second sampling interval are available. K-indexes characterising the geomagnetic activity in the middle latitudes are computed regularly. Main equipment of the observatory includes the digital variometer station TPM made in Poland (1996) and magnetoregistration device DI-fluxgate Magson gained on the co-operation bases with Geo Forshung Zentrum Potsdam and VW Stiftung. For absolute geomagnetic measurements,

the DI-fluxgate magnetometer and proton precession magnetometer ELSEC are employed. The magnetovariational data in the one-minute step are supplied via the internet to the INTERMAGNET centre. The data are sent to World Data Centers in Edinburgh and Paris, from where they are available for the whole geomagnetic and space weather community. The data are published also on the CD-ROMs prepared in the frame of INTERMAGNET. That is beacuse the Hurbanovo Geomagnetic Observatory GPI SAS is a member of INTERMAGNET, the international network of world first order magnetic observatories. Information about the geomagnetic activity is also published on the web site of the observatory, www.geomag.sk. The level of the geomagnetic activity si reported to public media (TV), too.

Old geomagnetic registrations of Hurbanovo Geomagnetic Observatory of GPI SAS (previous names of the observatory were Ógyalla and Stará Ďala) were rewritten to a digital form - bitmap pictures. Now, the data are available for the research of the geomagnetic field variations back to the beginning of the 20th century.

The members of the Hurbanovo Geomagnetic Observatory staff regularly perform field measurements at the observation points of the national magnetic repeat station network, which is a part of the European repeat station network. The measurements are coordinated by the MagNetE Group. Measurements of the magnetic declination are performed regularly at selected Slovak airports.

References:

1. REVALLO, M. - VALACH, F. - VÁCZYOVÁ, M. (2010). The geomagnetic storm of august 2010 as a lesson of the space weather modeling. In Contributions to Geophysics and Geodesy, vol. 40, no. 4, p. 313-322. (2010 - SCOPUS). ISSN 1335-2806.

2. VALACH, F. - REVALLO, M. - HEJDA, P. - BOCHNÍČEK, J. (2010). Predictions of SEP events based on linear filter and layer recurrent neural network. In 7th European space weather week, November 15-19, 2010: abstract book. Brussel: ESA, p. 69.

3. VALACH, F. - REVALLO, M. - HEJDA, P. - BOCHNÍČEK, J. (2010). Modelovanie kozmického počasia umelou neurónovou sieťou. In Zborník referátov z 20. celoštátneho slnečného seminára, 31. mája - 4. júna 2010, Papradno [elektronický zdroj] - Hurbanovo: Slovenská ústredná hvezdáreň, s. 162-168. ISBN 978-80-85221-68-8.

4. VALACH, F. - REVALLO, M. - HEJDA, P. - BOCHNÍČEK, J. (2011). Predictions of SEP events by means of a linear filter and layer-recurrent neural network, Acta Astronautica, Volume 69, Issues 9-10, 758-766.

5. REVALLO, M. - VALACH, F. - HEJDA, P. - BOCHNÍČEK, J. (2011). Geomagnetic Storm modeling by Means of Artificial Neural Network. In 8th European space weather week, 28.11. - 2.12. 2011: abstract book. - Namur, Belgium: ESA.

6. REVALLO, M. - VALACH, F. - BOCHNÍČEK, J.- HEJDA, P. (2011). Solar energetic particle flux as a measure of CME geoeffectiveness, 9. Slovenská geofyzikálna konferencia, 22.-23.6. 2011, Bratislava, Contributions to Geophysics and Geodesy.

7. VALACH, F. - REVALLO, M. - HEJDA, P. - BOCHNÍČEK, J. (2011). Solar energetic particle forecasts based on linear filter and layer recurrent neural network, 9. Slovenská geofyzikálna konferencia, 22.-23.6. 2011, Bratislava, Contributions to Geophysics and Geodesy.

In the ***Department of Astronomy, Physics of the Earth and Meteorology, Faculty of Mathematics, Physics and Informatics, Comenius University, Bratislava,*** the study of the effects of the solar proton flare (SPF) on the upper atmosphere response continued. ESF on July 14, 2000 was studied in terms of its effects on the Earth's atmosphere. Data of proton fluxes from satellite GOES-10 were used to calculate ionization rates. Concentrations of neutral as well as ion components were computed and their variations during SPF were examined. Changes in ozone after the SPF show a decrease of ozone of about 80% at altitudes of 65-75 km above the northern and 25% in a layer 55-65 km above the southern polar region. Observational data on [NO], [NO2], and [O3] from the UARS and HALOE satellites were used for comparison (and for 70° N have shown a good qualitative correspondence, however, for variations of nitric oxides there are quantitative discrepancies) (Kukoleva et al., 2010).

Solar activity influence on processes in the Earth's atmosphere was studied in terms of the Schumann resonance variations. By August 2009, SR measurements at AGO covered an interval of nearly 8 years, including both the solar cycle maximum and minimum. This enabled the SR frequency variability on the solar cycle time scale to be analysed. A decrease by 0.31 Hz from the latest solar cycle maximum to the deep minimum of 2009 is found in data from AGO. This extraordinary fall of the fundamental mode frequency can be attributed to the unprecedented drop in the ionizing radiation in X-ray frequency band. Although the patterns of the daily and seasonal variations remain the same in the solar cycle minimum as in the solar cycle maximum, they are significantly shifted to lower frequencies during the minimum. Analysis of the daily frequency range suggests that the main thunderstorm regions during the north hemisphere summer are larger in the solar cycle maximum than in the minimum (Ondrášková et al., 2011).

Since April 2007, dozens of sprites, optical transients above some +CG discharges, have been captured by automated all-sky TV system at AGO. As long continuing current in tens of ms in the parent +CG stroke radiates electromagnetic energy also in the SR band we analysed SR observations from Modra to find these ELF associates (counterparts). It was found that a majority (77%) of the optical transient events are accompanied with the transients in the SR band. No ELF counterparts are found for 23 % of the captured sprites. Our observations were verified by simultaneous observations in Sopron (sprites) and NCK (ELF counterparts). Our results suggest a possible difference between

parameters of the American and the European sprite producing +CG discharges (Ondrášková et al., 2010).

References:

1. ONDRÁŠKOVÁ, A. - ŠEVČÍK, S. - KOSTECKÝ, P. - TÓTH, J. - KYSEL R. (2011). On the relation between the red sprites and the transients in the ELF band, Contributions to Geophysics and Geodesy, 40 (2), 149-157.

2. KUKOLEVA, A. A. - KRIVOLUTSKY, A. A. - ONDRÁŠKOVÁ, A. (2000). Variations of the atmospheric chemical composition in the Earth's polar regions after Solar Proton Flare on July 14, 2000 (Photochemical Simulations), Cosmic Research 48, 1, 56-69.

3. ONDRÁŠKOVÁ, A. - ŠEVČÍK, S. - KOSTECKÝ, P. (2010). Decrease of Schumann resonance frequencies and changes in the effective lightning areas toward the solar cycle minimum 2008-2009. Journal of Atmospheric and Solar Terrestrial Physics 73, Issue 4, 534-543, DOI 10.1016/j.jastp.2010.11.013.

The activities of the ***Astronomical Institute of the Slovak Academy of Sciences*** (AISAS), Tatranská Lomnica (http://www.astro.sk), related to COSPAR, were devoted to the research in solar and stellar physics using different satellite observations, mainly in the UV, XUV and X-ray spectral regions. Stellar data of the IUE, FUSE, INTEGRAL satellites, and the HST were used for research of various variable stars [1,4]. Data of the current SOHO mission, the TRACE and the RHESSI satellites and previous satellites of the NOAA and GOES series were used for solar research [3,6,7,8]. Some other studies were focused on the solar activity with respect to the solar cycle and its influence on the heliosphere using the ground-based data [5] or on the possible interstellar meteors around the Earth [2]. Hereby we present some examples of the results obtained by the AISAS staff, an information on two education activities of the AISAS and a more extensive list of paper published by the AISAS staff related to the COSPAR activities.

Within the research of the stellar astrophysics, the data carried out with the space observatories, the X-ray Multi-Mirror Telescope (XMM-Newton), the Far Ultraviolet Spectroscopic Explorer (FUSE) and the Hubble Space Telescope (HST), were used to model the spectral energy distribution (SED) of symbiotic X-ray binaries (SyXBs). These exotic binaries comprise a cool giant or supergiant as the donor star and a white dwarf or neutron star as the accretor. Radiation of SyXBs dominates both the supersof X-ray and the far-UV domain. A fraction of the hot star energy is reprocessed into the thermal nebular emission, dominating the spectrum from the near-UV to longer wavelengths, and the donor star contributes significantly into the optical/near-IR (see Fig. 1). Therefore, to understand the nature of these objects, a multiwavelength approach in modeling their spectra is essential. First results on multiwavelength modeling the SED of SyXBs were presented at the conference on "Evolution of Compact Binaries" held at Vina del Mar, Chile 6-11 May 2011. Using own method of disentangling the composite spectra, fundamental parameters of individual radiative components were determined for a SyXB LIN~358 in the Small Magellanic Cloud (see Fig. 1). [4]

Intermediate polars (IPs) are a major fraction of all cataclysmic variables detected by INTEGRAL in hard X-ray. These objects have recently been proposed to be the dominant X-ray source population detected near the Galactic centre, and they also contribute significantly to X-ray diffuse Galactic ridge emission. Nevertheless, only 25% of all known intermediate polars have been

detected in hard X-ray. We used all observational data from INTEGRAL/JEM-X and INTEGRAL/IBIS to study possible variability of the selected IPs (V1223 Sgr and V709Cas) in the hard X-ray and soft γ-ray spectral bands. In addition, observations from INTEGRAL/OMC data were used to look for long-term variability of these objects in optical band. Our analysis showed that the fluxes of these IPs are long-term variable, mainly in the (15–25) keV and (25–40) keV bands. Moreover this hard X-ray/soft γ-ray variability is correlated with the changes in the optical spectral band in the case of V1223Sgr (Fig. 2). Our analysis revealed a deep flux drop around MJD ≈ 53 650 observed in both the X-ray as well as the optical band for this IP. [1]

A very close space around the Earth has been investigated by work performed in the Insterstellar department of the AISAS. The analysis of the 14 763 precise determined meteor orbits collected in the Japanese TV catalogue has called the occurence of interstellar meteoroids in the vicinity of the Earth into question, at least for meteoroids of masses corresponding to the video technique detections. The hyperbolic excesses of the heliocentric velocities were found in all cases about one order lower than required from the velocity distribution of neighbouring stars. The upper limit of the proportion of possible interstellar meteors to interplanetary ones among all investigated meteor orbits was determined to be 1.3×10^{-3}. [2]

We studied chromospheric evaporation mass flows in comparison with the energy input by electron beams derived from hard X-ray (HXR) data for the white-light M2.5 flare of 2006 July 6. The event was captured in high-cadence spectroscopic observing mode by SOHO/CDS combined with high-cadence imaging at various wavelengths in the visible, extreme ultraviolet, and X-ray domain during the joint observing campaign JOP171. During the flare peak, we observe downflows in the He I and O V lines formed in the chromosphere and transition region, respectively, and simultaneous upflows in the hot coronal Si XII line. The energy deposition rate by electron beams derived from RHESSI HXR observations is suggestive of explosive chromospheric evaporation, consistent with the observed plasma motions. However, for a later distinct X-ray burst, where the site of the strongest energy deposition is exactly located on the CDS slit, the situation is intriguing. The O V transition region line spectra show the evolution of double components, indicative of the superposition of a stationary plasma volume and upflowing plasma elements with high velocities (up to 280 km s^{-1}) in single CDS pixels on the flare ribbon. However, the energy

input by electrons during this period is too small to drive explosive chromospheric evaporation. These unexpected findings indicate that the flaring transition region is much more dynamic, complex, and fine structured than is captured in single-loop hydrodynamic simulations. [7]

The north-south asymmetries (NSA) of three solar activity indices are derived and mutually compared over the period of more than five solar cycles (1945 - 2001). A catalogue of the hemispheric sunspot numbers, the data set of the coronal green line brightness developed by us, and the magnetic flux derived from the NSO/KP data (1975-2001) are treated separately within the discrete low- and mid-latitude zones (5-30, 35-60). The calculated autocorrelations, cross-correlations, and regressions between the long-term NSA data sets reveal regularities in the solar activity phenomenon. Namely, the appearance of a distinct quasi-biennial oscillation (QBO) is evident in all selected activity indices. Nevertheless, a smooth behavior of QBO is derived only when sufficient temporal averaging is performed over solar cycles. The variation in the significance and periodicity of QBO allows us to conclude that the QBO is not persistent over the whole solar cycle. A similarity in the photospheric and coronal manifestations of the NSA implies that their mutual relation will also show the QBO. A roughly two-year periodicity is actually obtained, but again only after significant averaging over solar cycles. The derived cross-correlations are in fact variable in degree of correlation as well as in changing periodicity. A clear and significant temporal shift of 1-2 months in the coronal manifestation of the magnetic flux asymmetry relative to the photospheric manifestation is revealed as a main property of their mutual correlation. The reliability of the derived results was confirmed by numerical tests performed by selecting different numerical values of the used parameters. [5]

The Astronomical Institute organised in the year 2010 the lecture course - Modern Developments in Solar and Stellar Spectroscopy - given for the undergraduate and PhD studes from Slovakia, Czech republic, Poland by Prof. Kenneth Phillips, visiting professor of the Mullard Space Science Laboratory, affiliated with the University College London (UK) on May 17-21, 2010 at AISAS at Tatranska Lomnica. The course was focused on the basics of atomic physics and spectroscopy, spectra of the photosphere and chromosphere, and especially of the solar and stellar corona. The lectures aimed at showing how spectroscopy can be applied to determine physical properties (densities, temperatures, etc.) of solar coronal plasma as observed by SOHO, Hinode, and

other currently available instruments on-board space-borne satellites. In total more than 20 students took part in the course, and some staff members of the AISAS attended selected lectures. More details about the course of lectures can be found at the dedicated web page of the lecture course - http://www.astro.sk/~choc/open/10_kp_spec/10_kp_spec.html .

In the year 2012 another summer school was co-organized by the AISAS in its headquarters. The ISWI-Europe Summer School in Space Science at Tatranska Lomnica on August 21-27. The ISWI is a follow-up activity to the successful IHY 2007 but focusing exclusively on space weather. European scientists are successfully participating in the ISWI and many research level scientific instruments have been installed in many parts of Europe in the framework of the IHY and ISWI. In order to make maximum use of these and other similar initiatives and establish strong space research groups in Europe, a high level training of young students and researchers is very crucial. The summer school major objectives included teaching the fundamental knowledge and skills in space physics focuses on all research related mostly to the space weather. 46 students from 26 countries have taken part while to the total number of participants was 76. More details about the summer schools can be found at the web page of the school - http://stara.suh.sk/id/iswi/ISWI_School2011.htm.

References:

1. GÁLIS, R. - HRIC, L. - KUNDRA, E. - MÜNZ, F. (2011). Cataclysmic variables - X-rays and optical activity in V1223 Sgr and V709 Cas. In Acta Polytechnica : Journal of Advanced Engineering, vol. 51, no. 6, p. 13-16.

2. HAJDUKOVÁ, M., Jr. (2011). Interstellar meteoroids in the Japanese tv catalogue. In Publication of the Astronomical Society of Japan, vol. 63, p. 481-487.

3. HARRA, L. K. - STERLING, A. C. - GÖMÖRY, P. - VERONIG, A. (2011). Spectroscopic observations of a coronal Moreton wave. In *The Astrophysical Journal Letters*. ISSN 2041-8205, vol. 737, article no. L4, p. 1-6.

4. SKOPAL, A. (2011). Multiwavelength modelling the SED of symbiotic X-ray binaries. In Evolution of Compact Binaries: ASP Conference Series Vol. 447. Edited by Linda Schmidtobreick, Matthias Schreiber, Claus Tappert. - San Francisco: Astronomical Society of the Pacific, p. 233-238.

5. SYKORA, J. - RYBÁK, J. (2010). Manifestations of the North-South Asymmetry in the Photosphere and in the Green-line Corona, Solar Physics 261, 321-335.

6. UTZ, D. - HANSLMEIER, A. - MULLER, R. - VERONIG, A. - RYBÁK, J. - MUTHSAM, H. (2010). Dynamics of isolated magnetic bright points derived from Hinode/SOT G-band observations. In Astronomy and Astrophysics, vol. 511, article no. A39, p. 1-11.

7. VERONIG, A. - RYBAK, J. - GOMORY, P. - BERKEBILE-STOISER, S. - TEMMER, M. - OTRUBA, W. - VRSNAK, B. - POTZI, W. - BAUMGARTNER, D. (2010). Multiwavelength imaging and spectroscopy of chromospheric evaporation in an M-class solar flare. The Astrophysical Journal 719, 655-670.

8. VERONIG, A. - GÖMÖRY, P. - KIENREICH, I. W. - MUHR, N. - VRŠNAK, B. - WARREN, H. (2011). Plasma diagnostics of an EIT wave observed by HINODE/EIS and SDO/AIA. In The Astrophysical Journal Letters. ISSN 2041-8205, vol. 743, article no. L10, p. 1-7.

Figures:

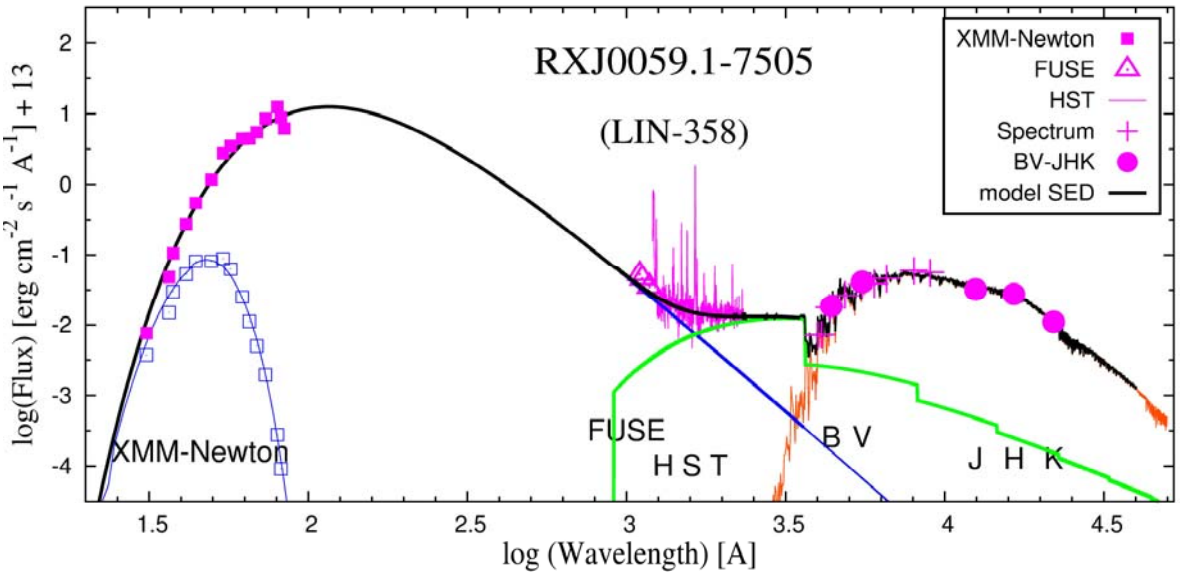

Fig. 1. A comparison of the measured (in violet) and modeled (heavy black line) SED of the symbiotic X-ray binary LIN~358 in the Small Magellanic Cloud.

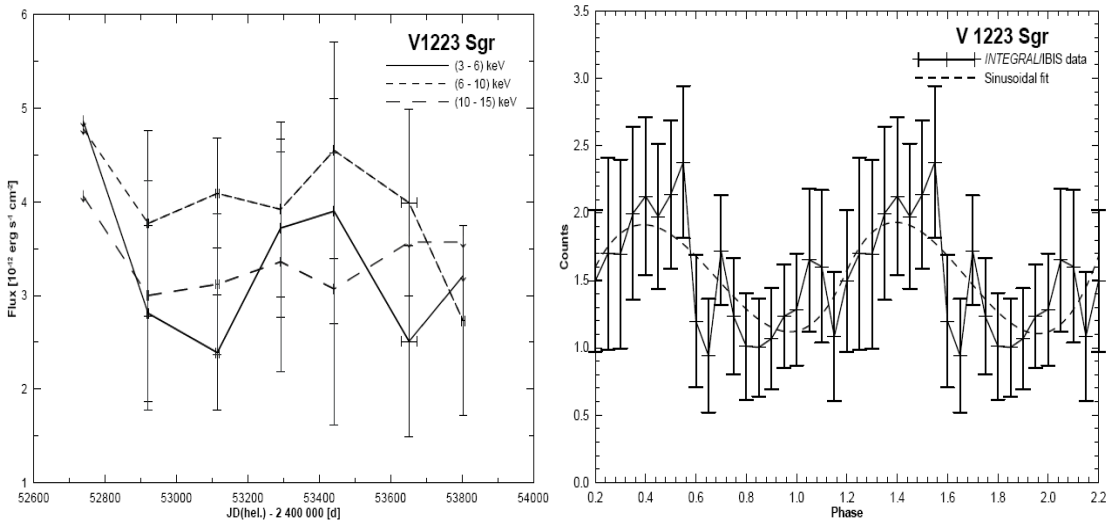

Fig. 2. Left panel: INTTEGRAL/JEM-X flux curves of V 1223 Sgr in the corresponding energy bands. The arrows represent 3 sigma upper limits. Right panel: INTEGRAL/IBIS phase diagram of V 1223 Sgr in (15-25) keV band floded with oprbital period (3.37 hrs).

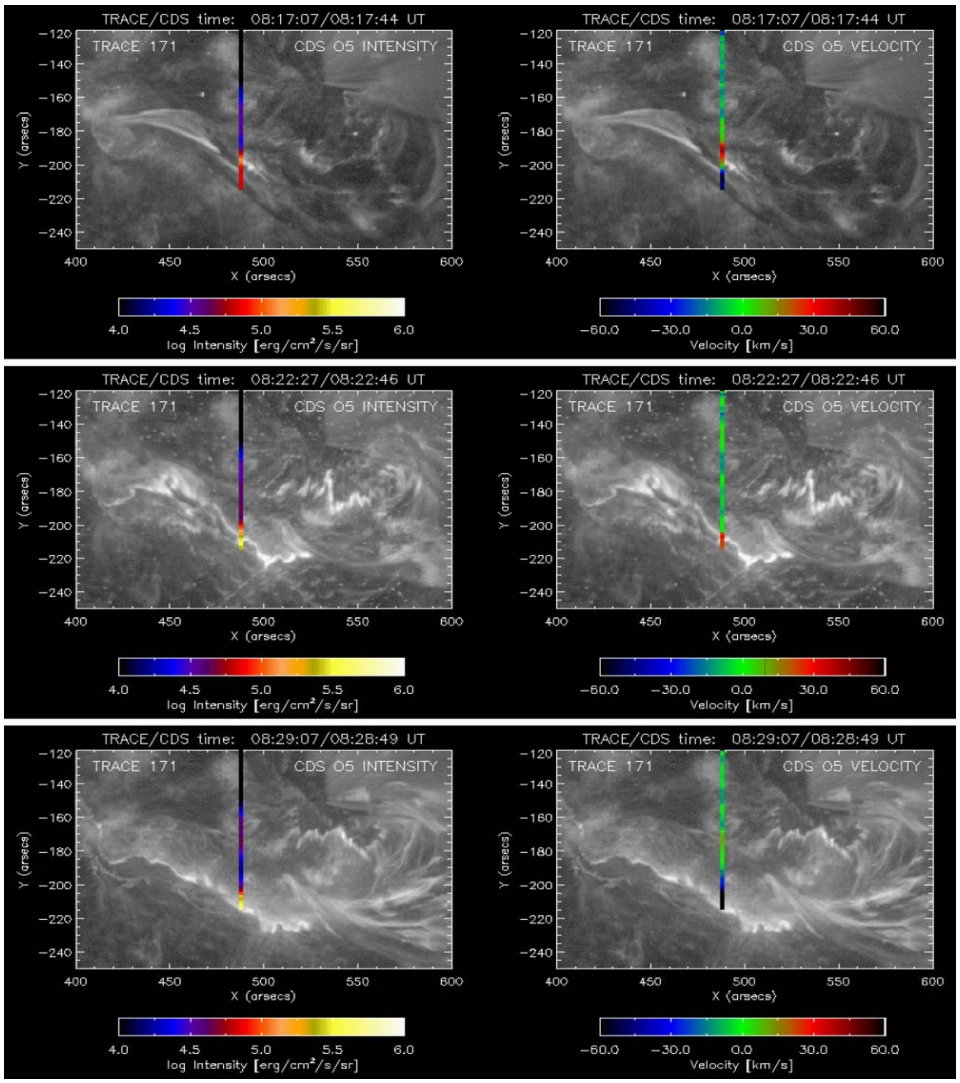

Fig. 3. Three snapshots of TRACE 17.1 nm images combined with the integrated intensities (left) and velocities (right) derived from the Gaussian fit to a co-temporal CDS spectrum in the O v line for the white-light M2.5 flare of 2006 July 6.. The top panel is taken during the time of the filament lift-off and commencement of the impulsive flare brightenings, the middle panel around the time of the highest HXR peak, and the bottom panel during the time of the distinct late RHESSI peak associated with the strongest transition region upflows at the CDS pixels crossing the flare ribbons.

3. MATERIALS RESEARCH IN SPACE

Material research activities in space of the ***Institute of Materials and Machine Mechanics of the Slovak Academy of Sciences*** (IMMS SAS) in the period 2010-2011 were focused on the international project (consortium of 6 partners) with ESA entitled "Gravity dependence of CET in peritectic TiAl alloys (acronym GRADECET)". The participation of IMMM SAS in the project is financially supported by the Slovak Academy of Sciences (SAS) in the frame of international cooperation of SAS with ESA.

The alloys of interest are peritectic TiAl based alloys that are excellent candidates for near net shape casting of light-weight structural components, like aero-engine blades (Fig. 1) or turbocharger wheels for automotive engines. These alloys are candidates to replace nickel based superalloy turbine components. Understanding the casting process of these alloys will lead to the production of a new generation of lightweight, fuel saving, aerospace turbine blades with lower density than conventional blades that can operate at even higher temperatures.

Fig. 1. Centrifugally cast low pressure turbine blades from TiAl based alloy by the coordinator of the project GRADECET - ACCESS, Germany.

Microgravity experiments offer a unique opportunity to study the effect of gravity on solidification of alloys. In microgravity conditions the effects of convection (thermal and solutal) are minimised and subsequently phenomenon associated with convection like sedimentation and macro-segregation, due to

fluid flow, are therefore removed. Performing identical ground based and hyper-gravity experiments and comparing results it is possible to examine the effects of gravity induced fluid flow during solidification, which will help to refine theoretical models of solidification.

One possible event in casting is columnar to equiaxed transition (CET). This occurs during columnar growth when equiaxed grains begin to form, grow, and subsequently stop the columnar growth. Normally either a columnar or equiaxed grain structure is desired in industry applications, so that consistent mechanical properties are achieved throughout the casting. During solidification, the CET of the primary phase leads to a change of the grain structure and hence to a change of mechanical properties. During columnar dendritic growth, grains align along the growth direction, leading to a pronounced crystallographic texture and to anisotropic mechanical properties. Columnar dendritic growth is targeted for example in Ni-base superalloys, in order to produce directionally solidified or even single crystal turbine blades. For most other castings, solidification with equiaxed grains is targeted, aiming to achieve isotropic properties throughout the cast part. The transition as such is hardly ever desirable. Therefore, understanding the conditions that produce the CET is of a great importance so that it can be avoided as necessary.

The project GRADECET is divided into three distinguished phases: (i) extensive ground based preparatory phase aiming at producing all necessary data and technical solutions for space mission, (ii) space mission using sounding rocket MAXUS and (iii) ground based evaluation of samples prepared at microgravity conditions.

Fig. 2 shows computer controlled Bridgman type of apparatus specially designed for ground based solidification and CET experiments of TiAl based alloys at the IMMM SAS [1]. The apparatus allows quenching during solidification (QDS) to preserve conditions at the solid-liquid interface and solidification experiments at controlled steady-state and un-steady state conditions. The un-steady state growth conditions are achieved by: (i) continuous change of the growth rate at a constant temperature gradient in liquid, (ii) continuous change of the temperature gradient in liquid at a constant growth rate and (iii) continuous change of both solidification parameters, i.e. temperature gradient in liquid and growth rate. The solidification experiments can be performed at various withdrawal rates ranging from 0.5 to

Fig. 2. Computer controlled Bridgman type apparatus designed for ground based solidification and CET experiments of TiAl based alloys.

4300 mm/h and the resistance furnace can operate at a maximum temperature of 1800 °C under vacuum or protective atmosphere. The apparatus allows direct measurements of temperature profiles, measurements of static and dynamic temperature gradients within the samples and thermal analysis of new alloys with unknown phase transformation temperatures.

One of the crucial tasks for the ground based and space experiments was to find suitable container material, which would resist to melted TiAl based alloys. Therefore, extensive evaluation of possible crucibles was carried out. Several types of oxide ceramics such as Al_2O_3, Y_2O_3 and CaO as well as combination of these ceramics with graphite crucibles showed that technically acceptable contamination of the samples can be achieved only with dense Y_2O_3 moulds. Based on numerous experimental measurements, activation energies and time exponents of kinetic equations for calculation of increase of oxygen content and volume fraction of ceramic particles as a function of the melt temperature and reaction time were determined [2].

Fig. 3 shows an example of cast macrostructure of large cast turbine blade from TiAl based alloy. The cast macrostructure consists of columnar grains growing from the surface toward the central region of the blade. Clear CET is visible between the columnar and equiaxed grain regions. Such

microstructural variations within the turbine blade lead to undesirable gradient of mechanical properties. Therefore, the industrial requirement is to avoid formation of CET within the cast blades and prepare castings with fine equiaxed grain structure. Fig. 4 shows an example of the Ti-46Al-8Nb (at.%) alloy prepared by directional solidification in Bridgman type apparatus [1]. The solidification at un-steady state growth conditions achieved by a continuous decrease of temperature gradient in liquid at a constant growth rate resulted in breakdown of columnar dendritic growth and formation of equiaxed grains ahead the columnar dendritic front. For the purpose of the GRADECET project, series of such CET ground based experiments for peritectic Ti-Al-Nb-B-C alloys are required at various combinations of growth rates and temperature gradients to construct CET diagrams. The ground based solidification data are used for the design and optimisation of resistance furnaces for parabolic rocket flight and selection of solidification parameters for microgravity CET experiments.

Fig. 5 shows furnace module which will be used in sounding rocket mission, MAXUS-9. The module is manufactured and commissioned by EADS Astrium. The module contains four integrated resistance furnaces working independently of each other.

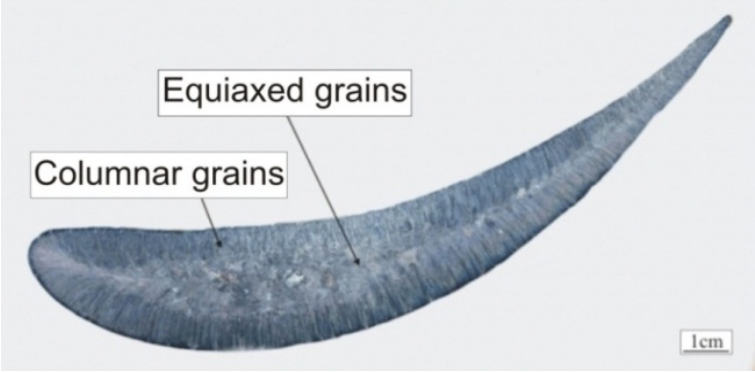

Fig. 3. Transversal section of cast turbine blade showing columnar grains growing from surface of the blade and equiaxed grains in the central region.

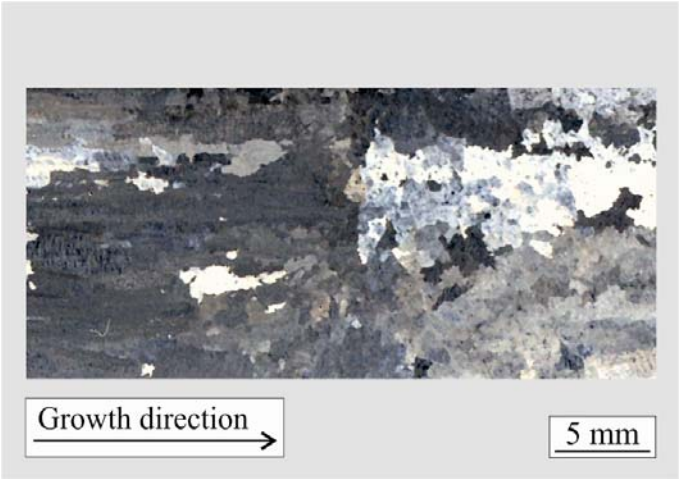

Fig. 4. Example of ground based experiment showing CET in Ti-46Al-8Nb (at %) sample prepared in the Bridgman type apparatus at controlled un-steady state growth conditions.

The furnaces are specially designed for TiAl based alloys and operate at a maximum temperature up to 1700 °C. Each furnace is equipped with three in-line resistance heaters [3]. The TiAl based alloy is enclosed in dense pureY_2O_3 crucible wrapped in a tantalum sleeve and outer tantalum cartridge. The cartridge is gastight and separated from the heaters compartment by helium so that the possibility of oxygen contamination is eliminated. The heater compartment is argon filled. For the reasons of mechanical stability and robustness, in the highly accelerated sounding rocket flight, the furnace module has no moving parts. Each

Fig. 5. Designed furnace module for sounding rocket mission MAXUS-9.

furnace has three thermocouples measuring temperatures fixed into the tantalum cartridge. The fourth thermocouple is fitted to the furnace to measure temperature along the axis of the sample.

ESA's next sounding rocket mission, MAXUS-9, is set to be launch in 2014 from the Esrange Space Centre just outside of Kiruna, Northern Sweden (Fig. 6). It will be carrying furnace module for CET experiments of peritectic TiAl based alloys. This campaign, using a MAXUS sounding rocket, will provide 12-13 minutes of stable weightless conditions. The MAXUS sounding rocket programme is funded by ESA through the European Programme for Life and Physical Science in Space (ELIPS) with the sounding rocket and launch services provided to ESA by an industrial joint venture between EADS Astrium and the Swedish Space Corporation. The payloads of the rocket will achieve an altitude of around 750 km (around twice the altitude of the International Space Station) before the descent back into earth's atmosphere begins. Along with the experiment modules the retrievable payload includes a parachute-based recovery system, a telemetry and telecommand module and a TV module. These microgravity experiments will be the foundation for advancement in production of new lightweight aircraft engine turbines as well as answering two fundamental research questions in materials science: (i) how does gravity affect the alloy's behaviour, as it transforms from liquid to solid and (ii) how does this shape the structure that forms during this solidification process. By varying different process parameters such as temperature gradients, it becomes possible to study other phenomena such as structural transition, segregation of alloying elements and effects of minor alloying elements on the grain refinement.

Fig. 6. Sounding rocket MAXUS.

References:

1. LAPIN, J. - GABALCOVA, Z. (2011). Solidification behaviour of TiAl-based alloys studied by directional solidification technique. Intermetallics, 19, 797-804.

2. LAPIN, J. - GABALCOVA, Z. - PELACHOVA, T. (2011). Effect of Y_2O_3 crucible on contamination of directionally solidified intermetallicTi-46Al-8Nb alloy. Intermetallics, 19, 396-403.

3. LEMOISSON, F. - McFADDEN, S. - REBOW, M. - BROWNE, D. J. - FROYEN, L. - VOSS, D. - JARVIS, D. J. - KARTAVYKH, A. - REX, S. - HERFS, W. - GROETHE, D. - LAPIN, J. - BUDENKOVA, O. - ETAY, J. - FAUTRELLE, Y. (2010). The Development of a Microgravity Experiment Involving Columnar to Equiaxed Transition for Solidification of a Ti-Al based Alloy. Materials Science Forum, 649, 17-22.

4. REMOTE SENSING.

Selected activities of four institutions are included to this report:

Institute of Geography, Slovak Academy of Sciences (IG SAS) in Bratislava participated in the **Urban Atlas** project. This is a joint project of the European Commission Directorate General (EC DG) for Regional Policy and EC DG for Enterprise and Industry. The work on this project consisted of the production of a series of land use/cover maps of larger urban zone (LUZ − selected 305 European cities have been interpreted). The satellite images (SPOT 5, RapidEye) of the reference year 2006 +/-1 were input data for this project.

The Urban Atlas aims to become part of a sustainable Global Monitoring for Environment and Security (GMES) Core Services that is continuously updated to find acceptance and ownership by local users, both in the public and private domain.

The task of IG SA together with IGN France International was external quality control of the interpretation products. The method used was a random oriented sampling according to a European grid and variable sample step, depending on the LUZ size.

All activities of the **Slovak Environmental Agency (SEA)** in Banská Bystrica were concentrated on the solution of **GMES** tasks. Obtained results are available on: http://seis.sazp.sk

Activities of the **Soil Science and Conservation Research Institute (SSCR)** in Bratislava were focused on the Control of area-based subsidies, Crop yield forecasting (regional inventory, monitoring of crop conditions and crop growth development, crop yield forecasting) and another images interpretations.

Remote sensing control of area-based subsidies in agriculture (2010-2011)

Slovak Administration decided to have six control sites for the 2010 campaign, defined by 20x20km in LEVO, LUCE, MART and SKAL, 15x15km in MICH and ZIAR. Five sites were covered by IKONOS images and one site was covered by GeoEye1 images. Two HR acquisition windows were used: HR-1 and HR+1.

The CAPI has been adjusted to the annual conditions of the regulations of subsidy schemes. Approximately 49 600 graphical annexes were printed and delivered to the farmers where they indicated the agricultural parcels they cultivate.

In 2010 campaign the total number of applicants was *15 984*, the number of dossiers controlled with remote sensing was *777* (4,86 % of all dossiers). The total area controlled was *99 216* hectares, with *5 463* reference parcels. There were *7 960* agricultural parcels to control (in 3 schemes), on average *10* parcels/farmer and *128* hectare/dossier.

According to the final diagnosis, which summarizes the diagnoses of the conformity and completeness tests at dossier level, 310 (39,9 %) dossiers were accepted for Single area payment scheme, 293 (37,7%) dossiers for Complementary National Direct Payment scheme and no dossier for Special Protection Areas (birds protected areas – Natura 2000). The subsidies play a key role in agriculture sector and contribute to the prosperity of agricultural subjects. The subsidies to agriculture sector represent major part of European budget and that's why there is taken an emphasis to the control.

Slovak administration decided to have five control sites for the 2011 campaign (Fig. 1): one defined by 15×15km square, two defined by 15×25km and 20×30km rectangle and two defined by 20x20km square:

- SITE 1 – PEZI (20×20km)
- SITE 2 – POBY (20×20km)
- SITE 3 – POLT (15×25km)
- SITE 4 – SNVE (20×30km)
- SITE 5 – VEKR (15×15km)

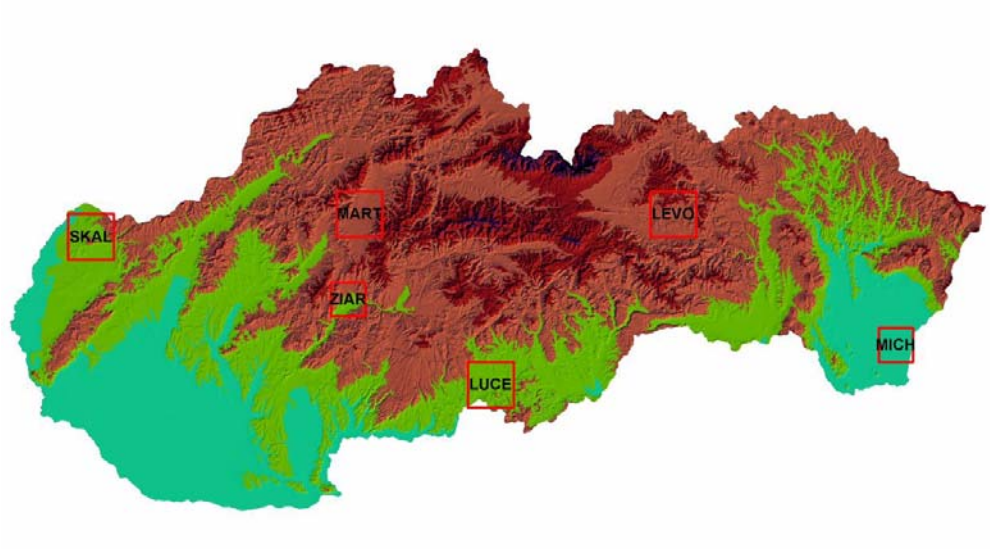

Fig. 1. Overview of the 2010 campaign sites.

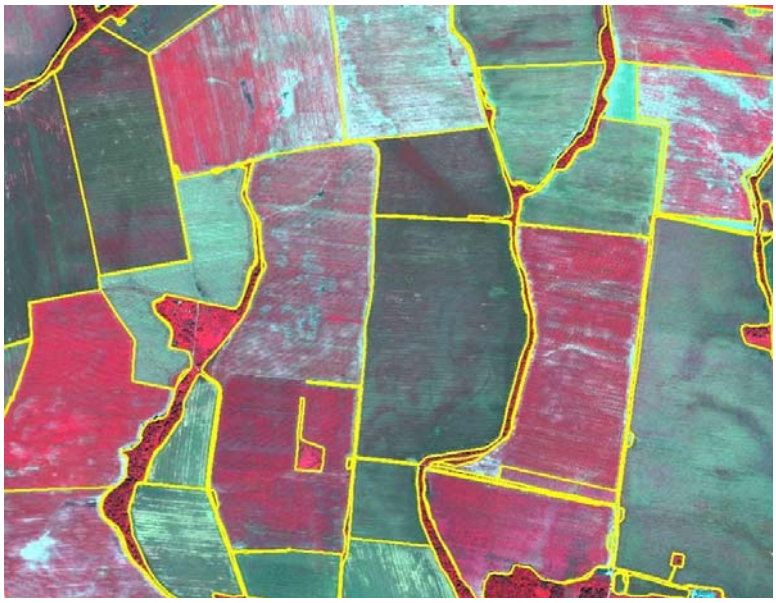

Fig. 2. Example of boundary check on GeoEye1 image.

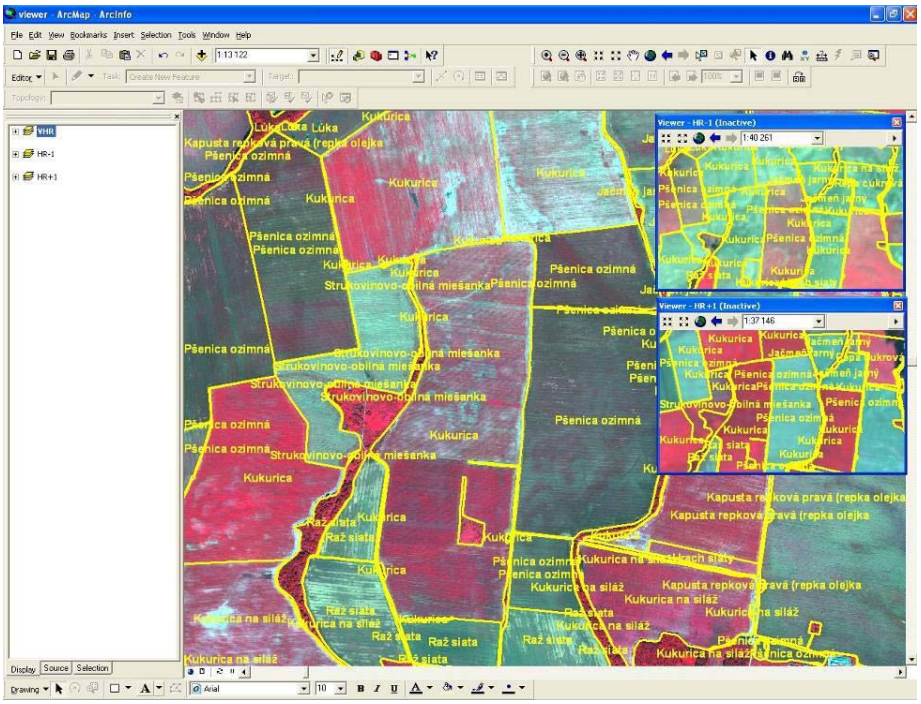

Fig. 3. Example of land use check on HR images from different acquisition windows.

Slovak Administration decided to have five control sites for the 2011 campaign, defined by 15×15 km in VEKR, 15×25 km in POLT, 20×20 km in PEZI and POBY, 20×30 km in SNVE. Four sites were covered by IKONOS images and one site was covered by WorldView2 image. Two HR acquisition windows were used: HR-1 and HR+1 (Figs. 2, 3).

The CAPI has been adjusted to the annual conditions of the regulations of subsidy schemes. Approximately *54 000* graphical annexes were printed and delivered to the farmers where they indicated the agricultural parcels they cultivate.

In 2011 campaign the total number of applicants was *16 087*, the number of dossiers controlled with remote sensing was *402* (2,50 % of all dossiers). The total area controlled was *34 869,67* hectares, with *2 061* reference parcels. There were *2 965* agricultural parcels to control (in 4 schemes), on average *7* parcels/farmer and *53* hectare/dossier.

According to the final diagnosis, which summarizes the diagnoses of the conformity and completeness tests at dossier level, 168 (41,79 %) dossiers were accepted for Single area payment scheme, 108 (26,87%) for Complementary National Direct Payment scheme and no dossier for Special Areas of Conservation and Special Protection Areas (for birds) (Fig. 4b).

Slovak administration decided to have five control sites for the 2011 (Fig. 4a) campaign: one defined by 15x15km square, two defined by 15x25km and 20x30km rectangle and two defined by 20x20km square:

- SITE 1 – PEZI (20x20km)
- SITE 2 – POBY (20x20km)
- SITE 3 – POLT (15x25km)
- SITE 4 – SNVE (20x30km)
- SITE 5 – VEKR (15x15km)

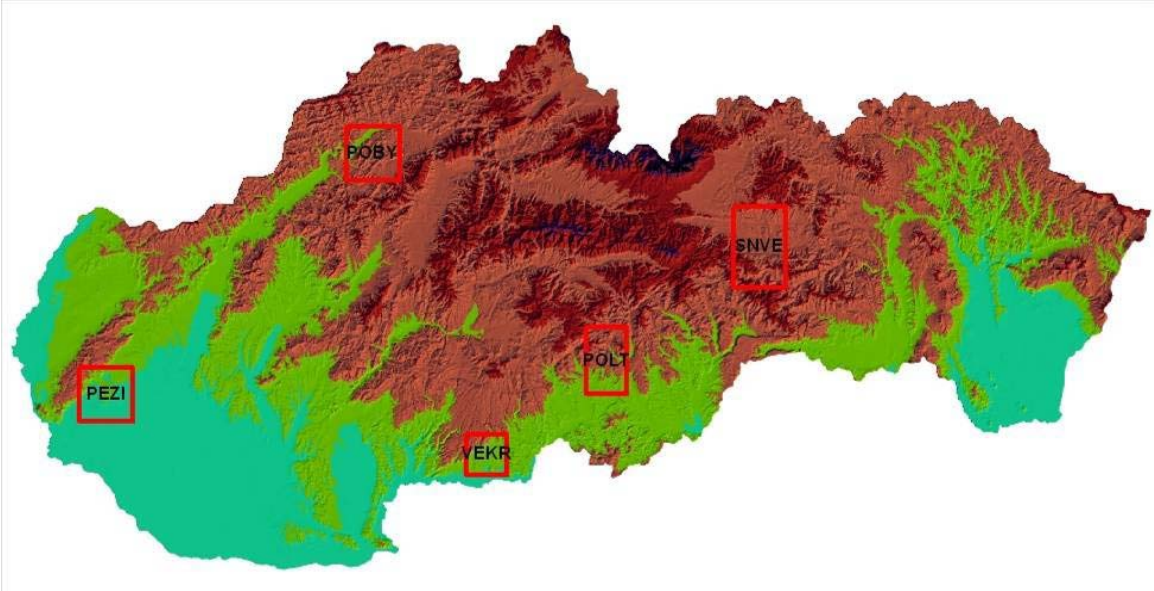

Fig. 4a. Overview of the 2011 campaign sites.

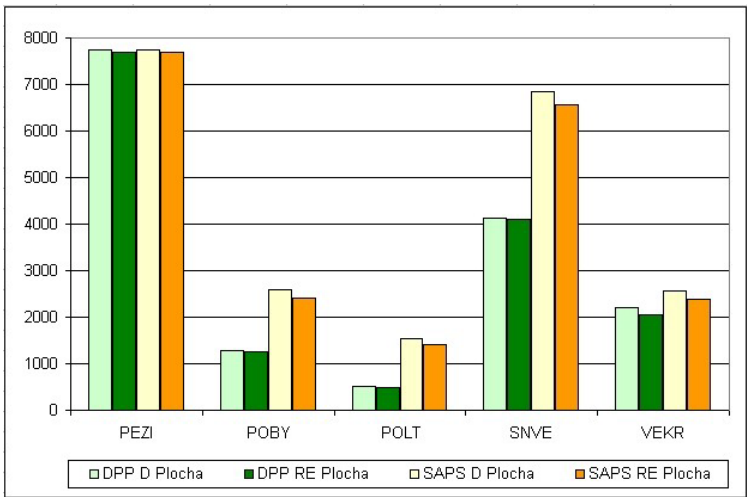

Fig. 4b. Declared and retained area (ha) for schemes CNDP and SAPS per site.

Monitoring of Crop Conditions and Crop Monitoring

Remote sensing within crop yield and crop production forecasting (2010 - 2011)

Monitoring of Crop Conditions and Crop Monitoring

Regional monitoring of natural crop conditions aims to study the influence of weather and soil on crop growth and crop development during current vegetation season.

Day and night land surface temperature, land surface moisture and also NDVI (Normalized Difference Vegetation Index) are derived from NOAA's AVHRR sensor (Figs, 5, 6, 7).

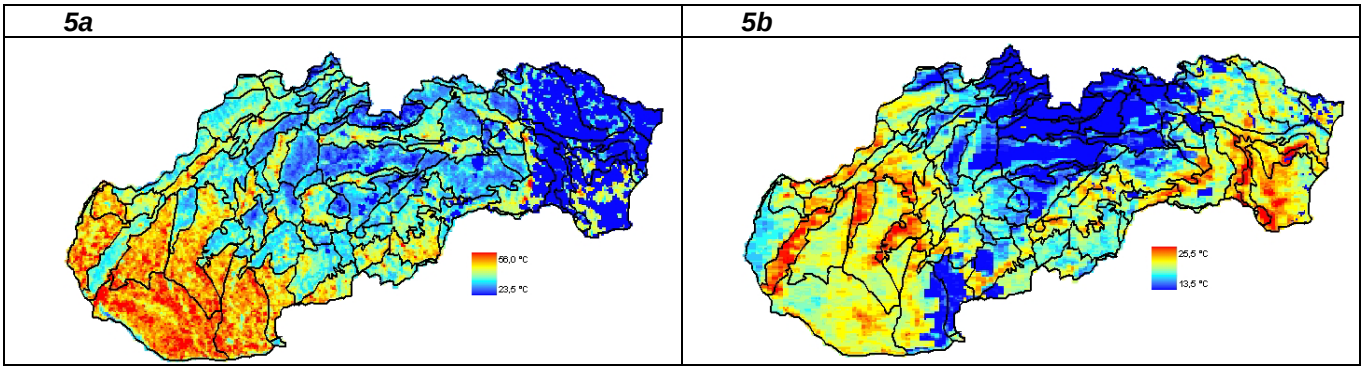

Fig. 5. Day (4a) and night land surface temperature average (4b) in the first decade of July 2010.

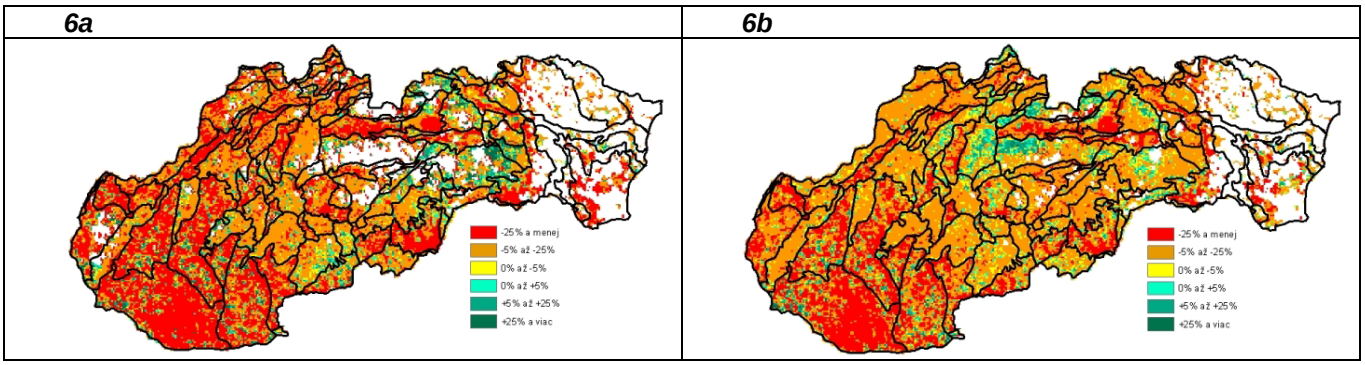

Fig. 6. Comparison of land surface moisture average in first decade of July in 2010 and in 2009 (5a); difference in land surface moisture average in first decade of July 2010 and long term average for the same period (5b).

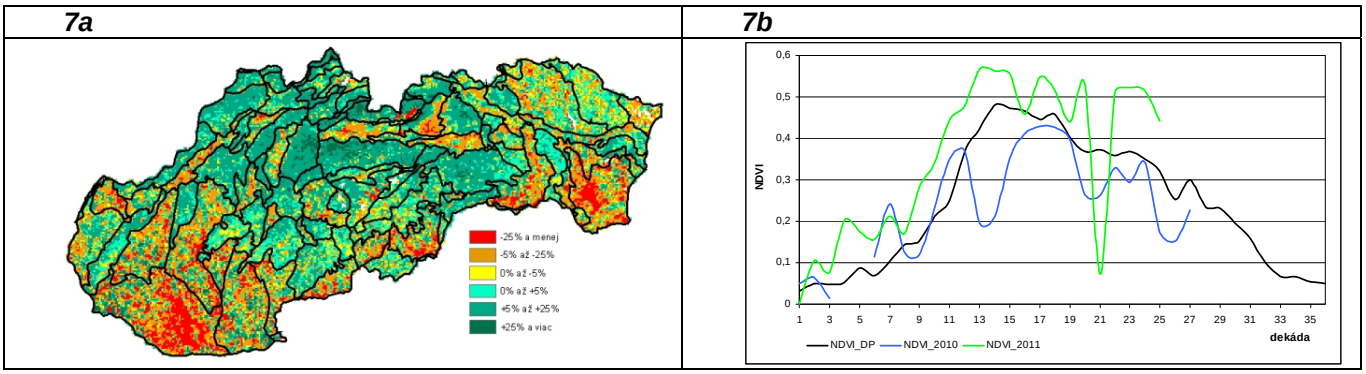

Fig. 7. Difference in NDVI in first decade of July in 2010 and NDVI long term average for the same period (6a); the figure with the comparison of NDVI development in 2011, 2010 and NDVI long term average (6b).

Crop yield forecasting

The aim of the crop yield and crop production forecasting is to provide the most likely, scientific, as precise as possible and independent forecast for main agricultural crop yields for Ministry of Agriculture of Slovak Republic and for the public.

National Crop Yield and Crop Production Forecasting System has been created on SSCRI and is based on two different principles which are applied to specify vegetation indexes as biomass stage and biomass development:

- Remote Sensing methods – interpretation of vegetation indicators (as NDVI or DMP- Dry matter development) from satellite images (mainly from low resolution satellite sensors as NOAA AVHRR and SPOT Vegetation satellite system;
- Bio-physical modeling (WOFOST model) and simulation of vegetation indexes (mainly TWSO - Total Dry Weight of Storage Organs and TAGP - Total Above Ground Production). In WOFOST, weather and phenological data, soil hydro-physical data and crop physiological data are utilized as model key inputs;
- Integrated assessment method, which means the implementation of specific meteorological and vegetation indicators in the statistical analysis, assesses the impact of weather on the projected

harvest. Integrated estimate summarizes a wider range of disparate indicators and indices that are currently for the purposes of forecasting yields and consequently the production of crops used.

The crop yield and crop production forecasting is carried out for main agricultural crops – winter wheat, spring barley, oil seed rape, grain maize, sugar beet, sunflower and potatoes. The forecasts are reported six times per year – in the half of May, June and July for "winter and spring crops" and in the end of July, August and September for "summer crops". The forecast results are interpreted at national level as well as at NUTS 3 and NUTS4 level. The example crop yield forecasting in 2011 can be seen in the Fig. 8.

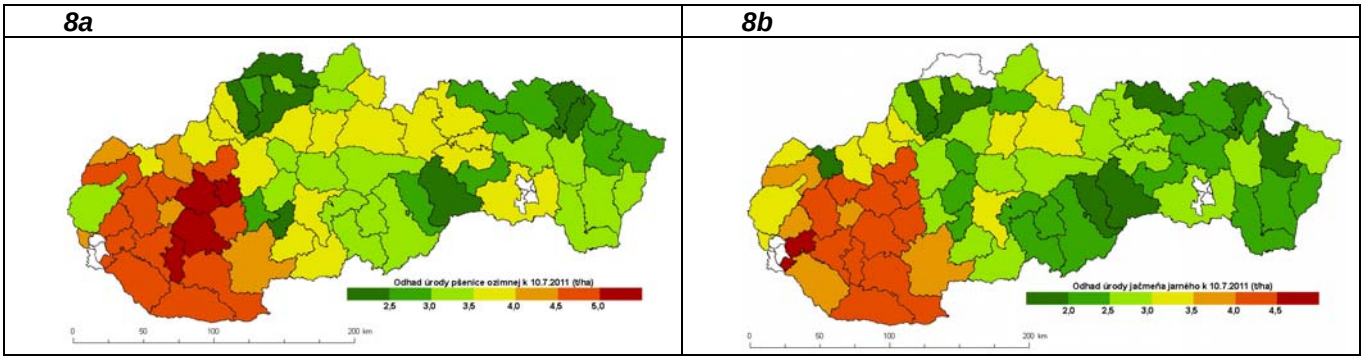

Fig. 8. Example of crop yield forecasting with remote sensing in first decade of July in 2011: winter wheat (7a) and spring barley (7b).

Remote sensing research activities of the **National Forest Centre (NFC)** in Zvolen were solved in the framework the project *Centrum of excellence for decision support in forest and countryside*[1]. The research was aimed at two basic topics:

- Application satellite-based observation of forest ecosystem's response to global environmental changes.
- Research of the methods of classification and structural models of favourable state of forest ecosystems in Slovakia using Remote Sensing

The significant progress was achieved in the following areas:

[1] This work was supported by Operational Programme Research and Development in framework of the project *Centrum of excellence for decision support in forest and countryside*, ITMS 26220120069.

Assessment of drought impact on Turkey oak stands using MODIS satellite imagery

The research has been aimed at response of forest vegetation to the occurrence of climate extremes. Intra-seasonal variability of vegetation index was derived from MODIS instrument (Moderate Resolution Imaging Spectroradiometer). The presented results were obtained in the permanent forest monitoring plot Čifáre in 2003; this year was selected because of extreme drought that occurred. The plot is occupied by Turkey oak (*Quercus cerris*). The 23 satellite records were acquired and time series of NDVI (Normalized Differentiated Vegetation Index) were created. This series has been translated sigmoidal function that suitably approximates intra-seasonal course of the NDVI. Consequently, differences between observed and fitted values (residuals) were calculated. The negative values of residuals are thought as vegetation stress responses to environmental factors. The distribution of negative residual are interpreted in relation to periods of drought and heat waves. A decrease in NDVI in magnitude of 3-10%, as compared to the value at the beginning of the sequence of negative residuals, was observed. Although such responses are not too large, it is possible to visually evaluate their association with the occurrence of investigated climatic extremes (Fig. 9) (Hlásny et al. 2011).

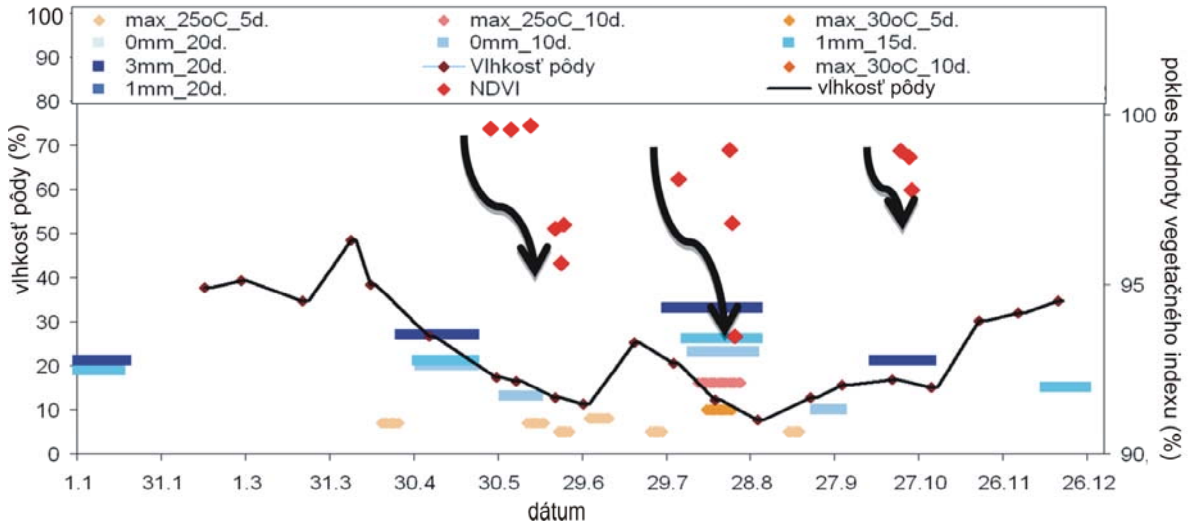

Fig. 9. The observed sequence of NDVI in Turkey oak stand in Čifáre plot in relation to the occurrence of selected climatic extremes.

All observed changes were reversible, and after the first period of rainfall the NDVI values returned to the baseline level. These finding confirmed the sensitivity of satellite-derived vegetation index on the occurrence of climatic extremes, and feasibility of such approach for the assessment of climate effects upon the vegetation.

Modeling phenological development of forest vegetation using NDVI index derived from MODIS satellite imagery

The research brings a new innovative approach for estimation of phenological events of forest stands from satellite spectroradiometer MODIS. We focused on spring-time vegetation sprouting buds and leaf unfolding (Fig. 10). Normalized vegetation index (NDVI) was used to determine the onset of the vegetation stages. Sigmoid curve [1] was applied to shape a course of NDVI:

$$v(t) = v_{\min} + v_{amp}\left(\frac{1}{1+e^{m_1 - m_2 t}} - \frac{1}{1+e^{m_3 - m_4 t}}\right) \qquad [1]$$

The software product Phenological profile was developed for this purpose. It allows to calculate the value of extremes of the function for spring and autumn phenophase as well as to determine the date on which occur. In the period 2000-2010, the earliest start of leaf unfolding was observed in 2009. The median value was 110 day of the year and took from 104 to 122 day for 5–95% quintile. The latest start was observed in 2010, and took from 114 to 135, median = 121 day. Leaf unfolding is delayed non-linear with the increase of altitude. Unfolding is shifted by 0.4 day between heights 200 and 300 m a.s.l. A shift is 7.6 day between heights 1200 and 1300 m a.s.l.

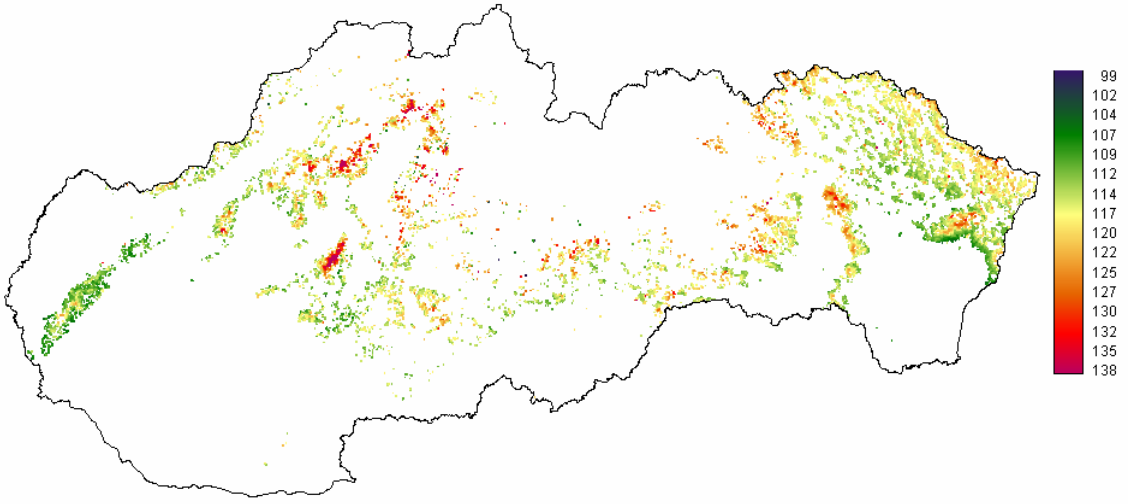

Fig. 10. Day of year of onset of phenophase leaf unfolding. The mean value from period 2000–2010 of beech stands. The mean corresponds to an inflection point of function.

The application of satellite images for documentation and development of spruce decline

The research dealt with an assessment of spruce decline using satellite imagery from Landsat at national level and in small-scaled protected areas as well (Fig. 11). Two-phase regression sampling method was applied to assess of spruce forest condition in 2000 and 2010. These two classifications were mutually compared on both national and protected areas level. The classifications show that area of damaged spruce forest increased from 11.3 % in 2000 to 16.1 % in 2010. This worsening was even higher in small-scaled protected areas (4^{th} and 5^{th} level of protection) where portion of damaged spruce forest increased from 11.0 % to 23.1 %. It raises questions about suitability of non-intervention regime and about future management of protected areas. The results confirm that spruce is endangered in all area of its occurrence caused by a concurrent impact of biotic, abiotic and anthropogenic injurious agents.

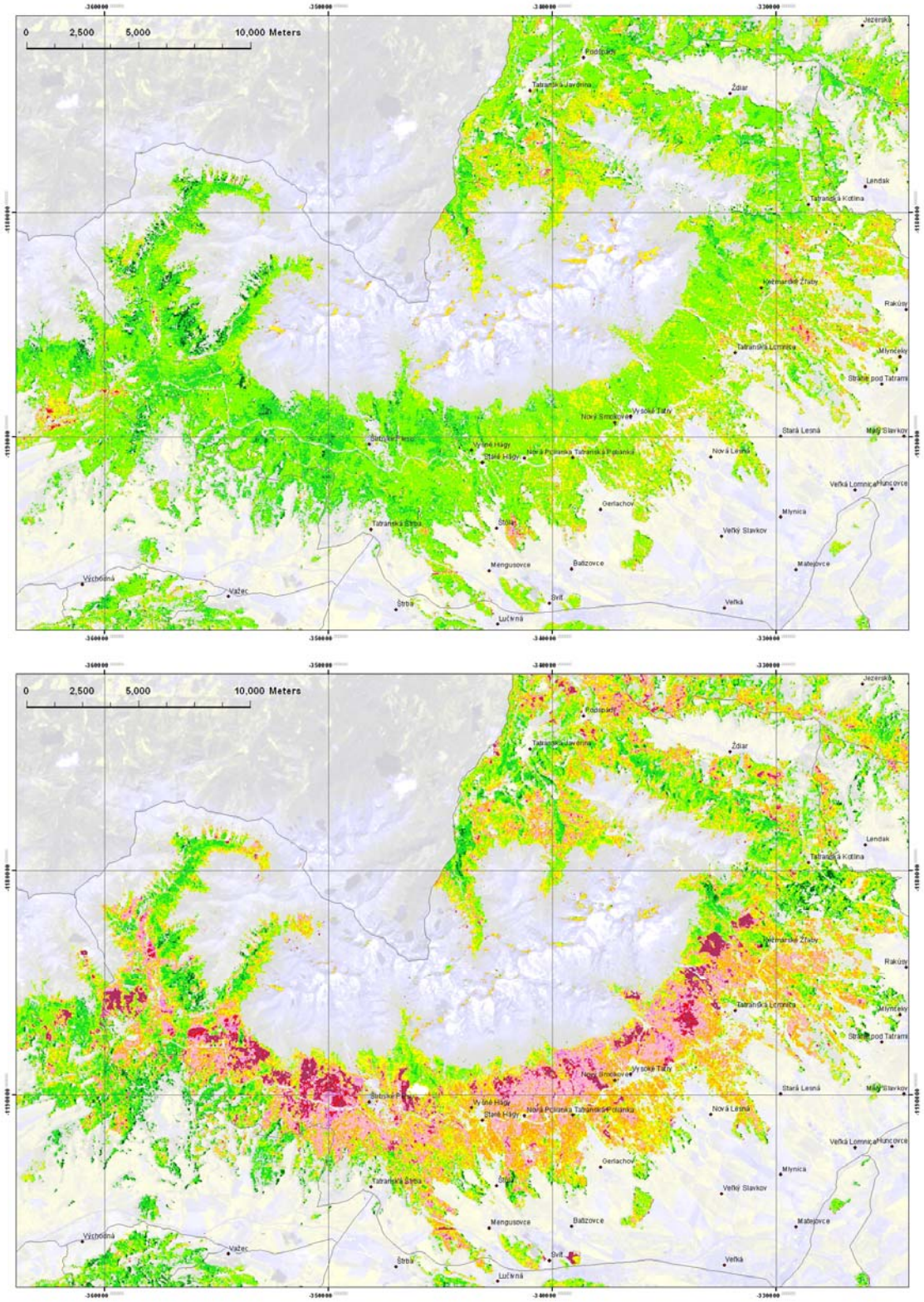

Fig. 11. Classification of spruce stand's damage in 2000 (top) and 2010 down in the Tatra National Park from Landsat satellite images. Size ~ 40 x 27 km. Colour scale interpretation: from dark green to purple = from healthy to died forest stands.

Development of satellite-based system for a continuous evaluation of forest's response on changed environmental condition: Structure of information system

Structure of the information system was evolved by gradual development and optimization. IS compounds of two subsystems aimed at health (Landsat, SPOT and Aster – high resolution satellite data) and ecological and productive state of forest (MODIS – medium resolution satellite data). Each subsystem has its own tools for data pre-processing, storage, analyses and publication (Fig. 12).

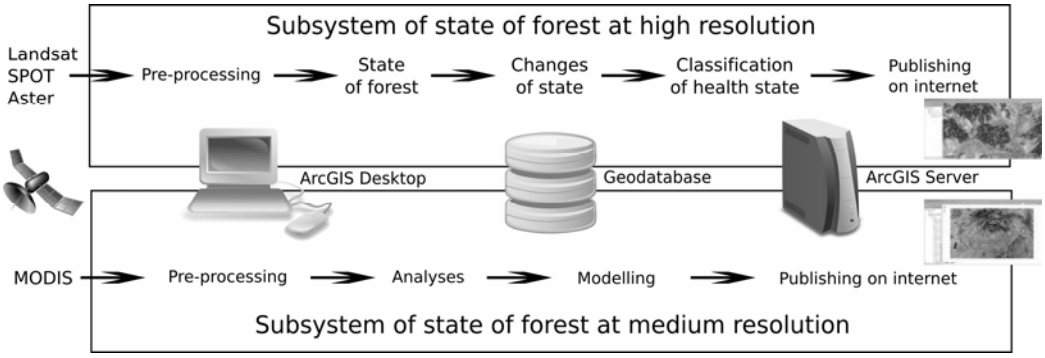

Fig. 12. Structure of satellite-based system for a continuous evaluation of forest's response on environmental condition.

The 1st subsystem is proposed to inform forest owners and forest state administration about the actual state of forest stands and its changes (Fig. 13).

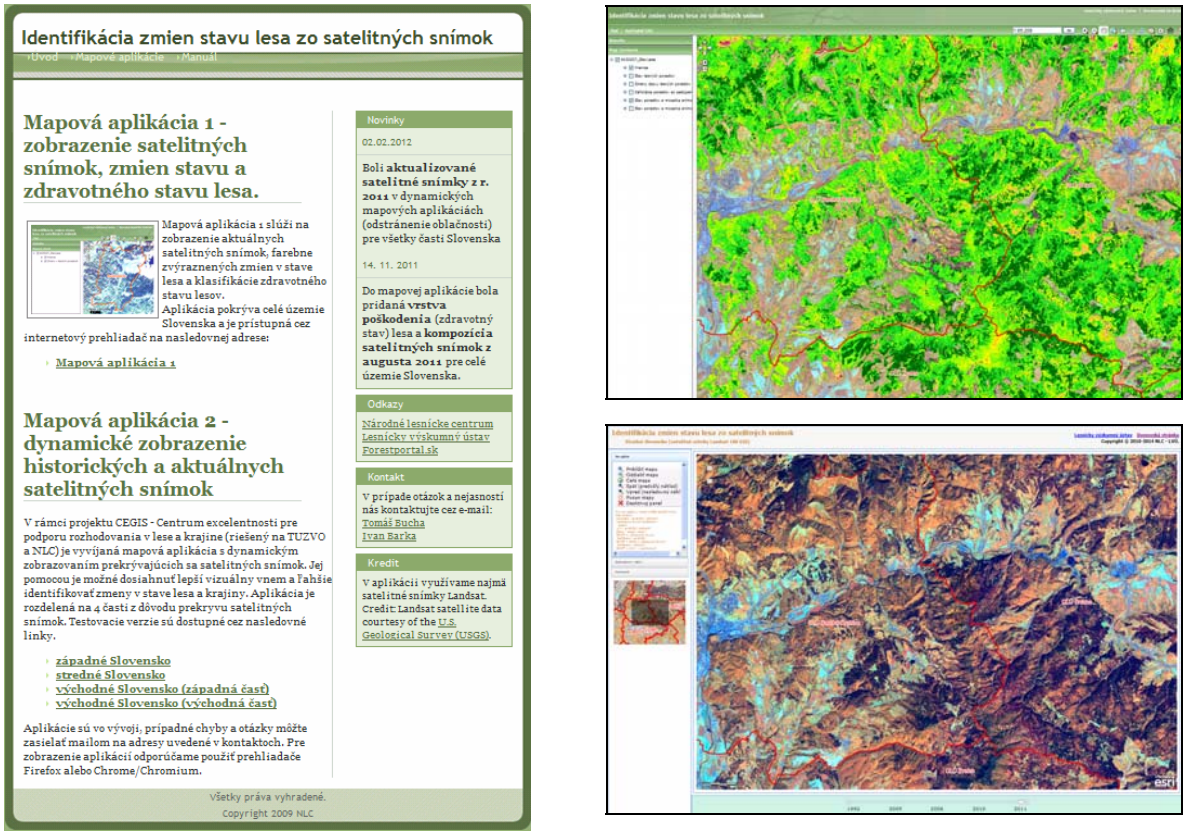

Fig. 13. Left: Web application (http://www.nlcsk.org/stales/) focused on state of forest stands. Right - top: Map application 1: Classification of forest health condition in 2011 from Landsat. Right - bottom: Map application 2: Dynamic view of Landsat composites since 1994 to 2011.

Credit: Landsat satellite data courtesy of the U.S. Geological Survey (USGS).

Research of the methods of classification and structural models of favourable state of forest ecosystems in Slovakia using remote sensing (http://strumodekos.nlcsk.sk/)

The new approaches in both the thematic mapping and classification of forest structure were investigated. Object-oriented approach allowed to create and to propose a methodological framework for the description of forest landscape in complexity of the variability in tree species composition, diversity of the stand structure conditioned by the development process as well as forest-economic activity of man. The forest landscape mapping system at stand and tree level was elaborated on example: 1) stand texture typified by methods of visual interpretation of segments delineated from Landsat satellite scenes at different hierarchical levels; 2) automated (digital) classification of segments into stand texture types from the viewpoint of health state (managed forests) and development stages (natural forests), based on Ikonos satellite scenes with 1 m

spatial resolution; 3) derivation of the structural characteristics of forest stands (percentage of coniferous and deciduous trees in the stand type, their spatial distribution and vertical layout) from multispectral aerial images with very high resolution of 0.2 m (Figs. 14 and 15). Innovativeness of the solution lies in the proposed concept of a hierarchical, object-oriented forest typification based on the stand textures.

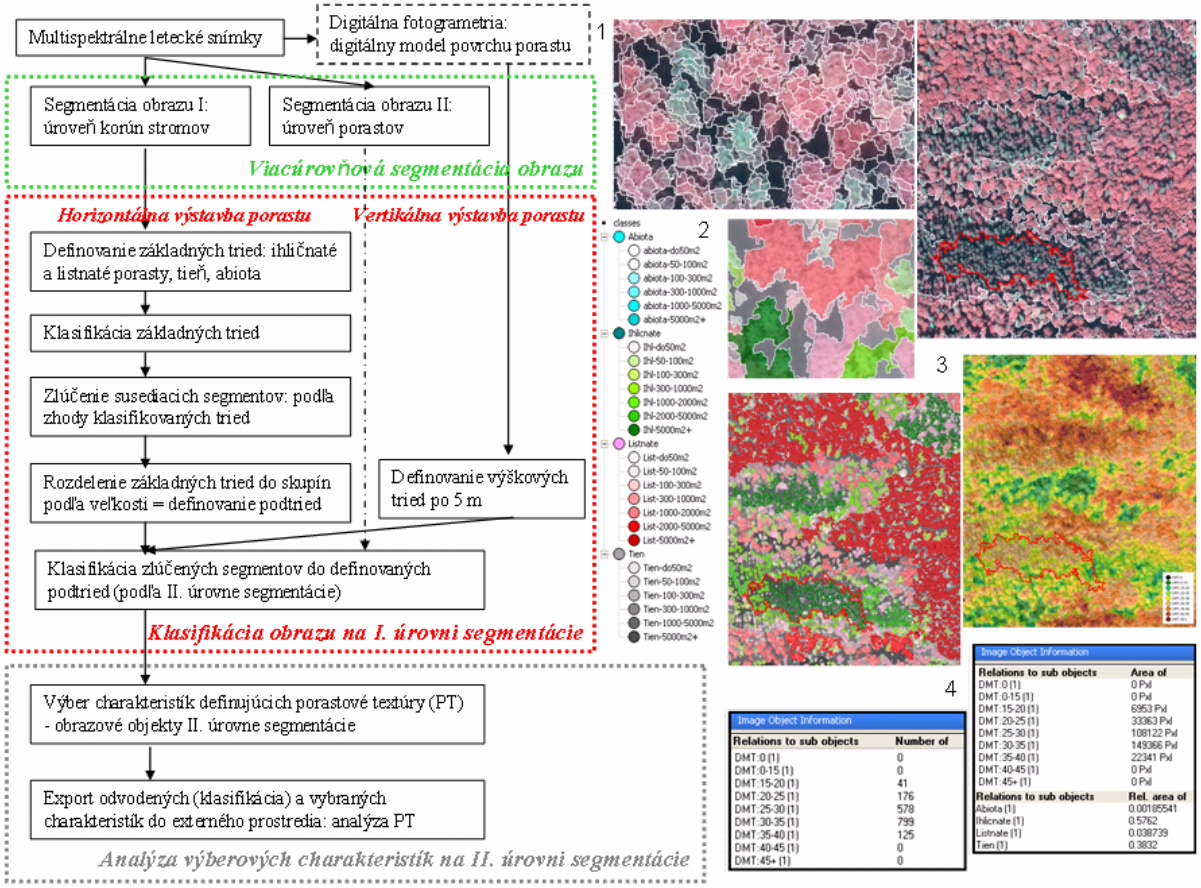

Fig. 14. Left: The concept of derivation of the structural elements of forest stands from aerial imagery. Right: graphic documentation of steps with using multispectral aerial imagery:
1. Step: Image segmentation in two levels (crown and stand level),
2. Step: Class definition (coniferous, deciduous, shades and abiotic elements), image classification and merging adjacent identical categories;
3. Step: Merging categories into groups according to their size;
4. Step: Numerical summaries of the derived variables (example of vertical structure differentiation) according to 2nd level of segmentation.

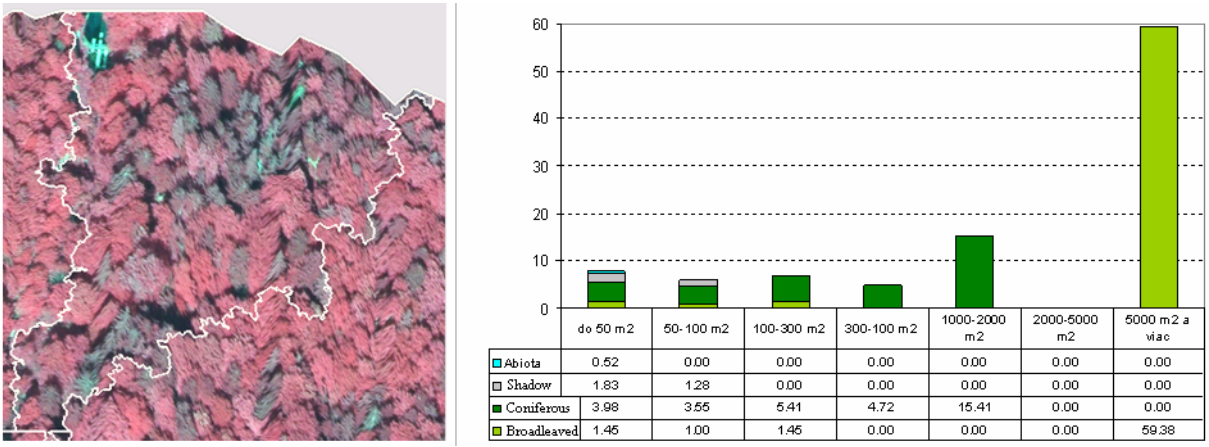

	do 50 m2	50-100 m2	100-300 m2	300-100 m2	1000-2000 m2	2000-5000 m2	5000 m2 a viac
Abiota	0.52	0.00	0.00	0.00	0.00	0.00	0.00
Shadow	1.83	1.28	0.00	0.00	0.00	0.00	0.00
Coniferous	3.98	3.55	5.41	4.72	15.41	0.00	0.00
Broadleaved	1.45	1.00	1.45	0.00	0.00	0.00	59.38

Fig. 15. Left: multispectral aerial image – typical texture of old forest stand: Fir and beech stands with spruce. Right: Percentage of classified categories (deciduous, coniferous, shadow, abiotic elements) by the size groups in the segment. The sum represented = 100%.

5. SPACE METEOROLOGY.

SHMÚ has continued in the cooperation with EUMETSAT in the frame of H-SAF project (Satellite Application Facility on support to operational Hydrology). After five years of the products development by consortium partners (2005-2010) project continued from September 2010 with operational and continuous development phase (CDOP). Main task was to validate existing precipitation products whether or not they satisfied with the user requirements. Radar precipitation measurements with the combined ground based precipitation data were the main validation data used in the SHMÚ. For this purpose we combined rain gauge data and NWP (Numerical Weather Prediction) model outputs with radar data. Combination was done by system INCA (Integrated Nowcasting through Comprehensive Analysis). In SHMÚ we have developed set of source codes for bulk validation parts of which were adopted by the whole H-SAF consortium. Main features of validation procedures there are up-scaling of radar data into native satellite grid matching the ground truth and the satellite data in time and space and finally the calculation of statistical scores which can be used to evaluate the product quality (Figs. 1 and 2).

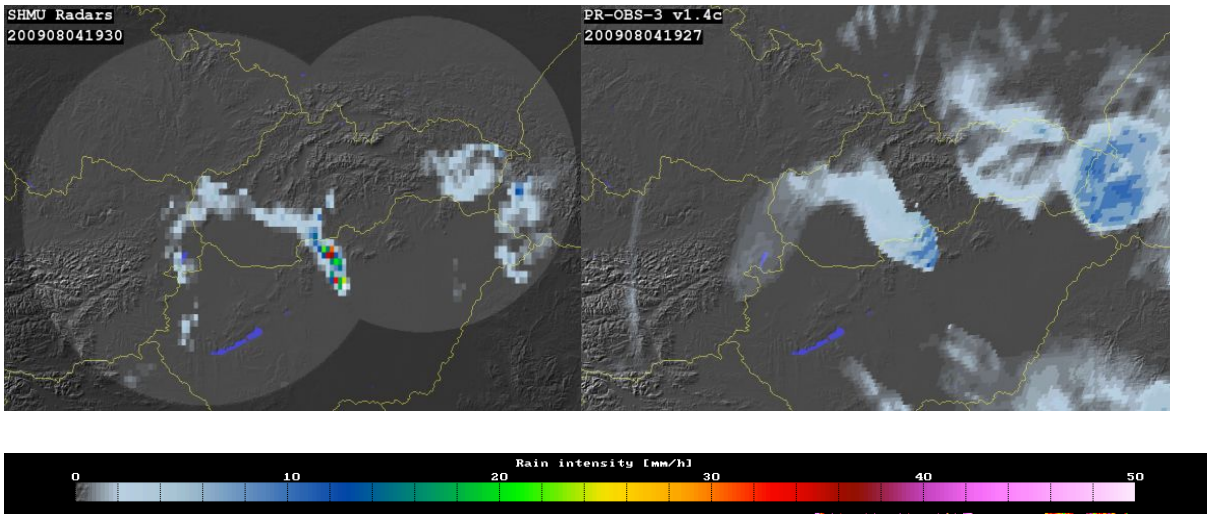

Fig. 1. Comparison of rain intensity detected by SHMÚ radar network (left) and H-SAF PR-OBS-3 product (right) for 4th August 2009, at 1930 UTC. Main objectives of validation there are spatial consistency, capability to detect higher precipitation intensities of extreme precipitation events and capability to detect short-time changes of convective (fast developing) precipitation. PR-OBS-3

product represents instantaneous precipitation maps generated by IR images from operational geostationary satellites "calibrated" by precipitation measurements from MW images in sun-synchronous orbits, processed soon after each acquisition of a new image from GEO ("Rapid Update").

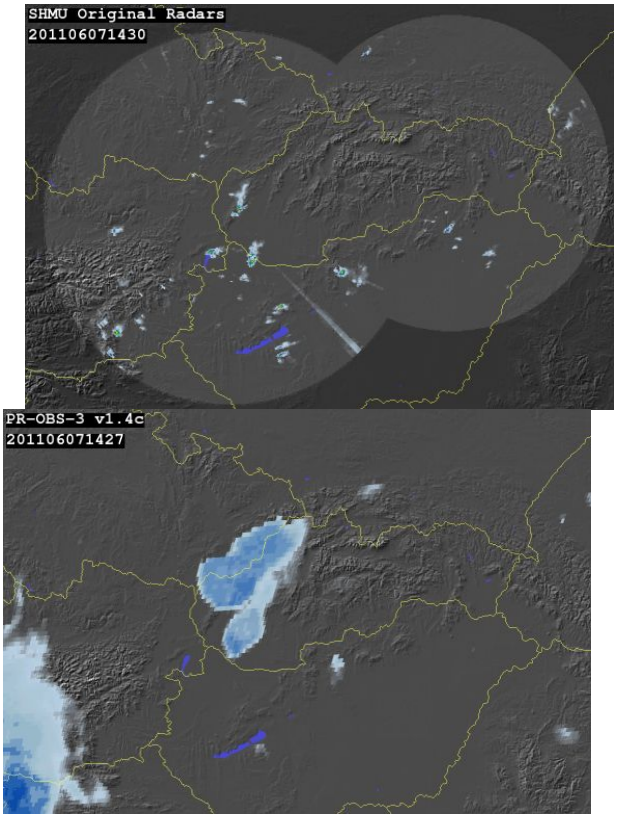

Fig. 2. Flash floods in villages under Little Carpathians slope: Comparison of rain intensity detected by SHMÚ radar network (left) and H-SAF PR-OBS-3 product (right). Main problem still holding over satellite sensors there is low space resolution and space inconsistence in precipitation distribution and resulting drop-out the precipitation extremes. Satellite data defectives are studied in validation process and this information is provided as feedback to product developers.

SHMÚ uses the Nowcasting SAF software for operational generation of several products, which are used for current weather analyses, nowcasting and very short range forecasting. Applications enable to use meteorological satellite data optimally. Cloud types, cloud top parameters (temperature, pressure and height), probability of precipitable clouds and layer precipitable water are the main products which support nowcasting (Fig.3).

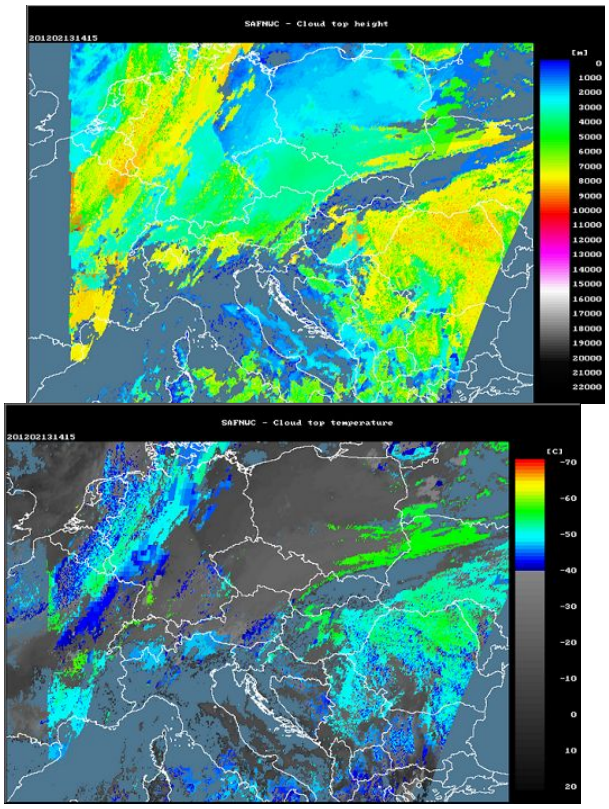

Fig.3. Nowcasting SAF products – Cloud top height (left) and Cloud top temperature (right) are useful for analyses of current weather situation, especially for aviation control and during summer for severe storms detection.

For the air mass analyses there are products based on IR imagery and temperature / humidity vertical profiles: total precipitable water, layer precipitable water (for bottom, medium and high tropospheric layers) and stability analyses indexes, which serves to detect potential of convection and storm development during summer season.

To extend the set of stability indexes we have developed and implemented new stability index – dThetaE2 [K], which can be used as complementary parameter to K and Lifted indexes and increase the reliability of air mass stability estimation (Fig. 4.).

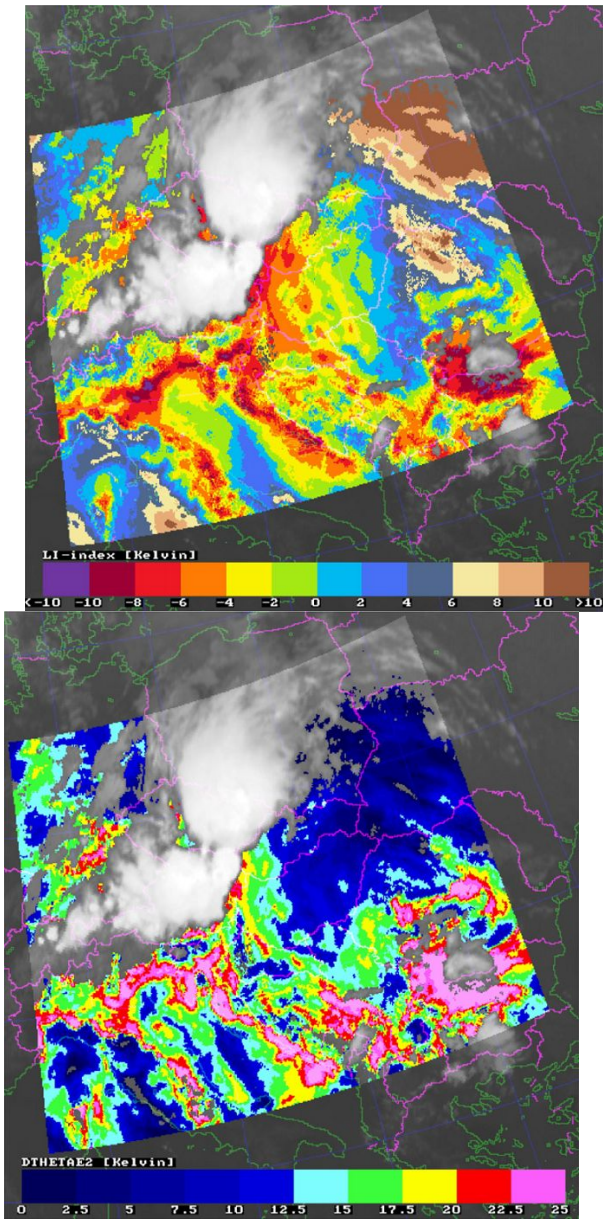

Fig. 4. Left: The composite image of LI-index [K] over clear areas and MSG IR 10.8 μm channel (over cloudy areas) at 1915 UTC, 25 June 2008. Right: The same as in left, but for new dThetaE2 index [K], which is more sensitive to air instability.

SHMÚ is the member of EUMETSAT Convection Working Group which was established with the aim to collect tools, ideas, algorithms and methods for the best utilization of satellite data for detection of convection connected with severe weather like thunderstorms, heavy precipitation, wind gusts, hail and lightning. SHMÚ is sharing skills with this group in localization of overshooting tops of severe storms in satellite imagery, detection of storm's top structure, estimation of their heights, study on distribution of storms over central Europe in dependence of season, day time and sun height (Figs. 5 and 6). Investigations

are based on MSG satellite data received and archived from May 2008 until present days.

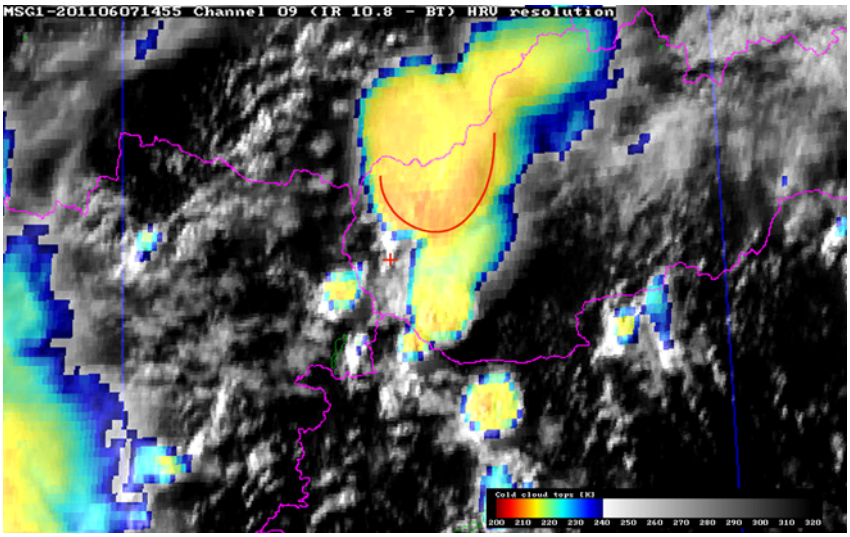

Fig. 5. Storms in Little Carpathians slope hided Častá, Píla and other villages and surroundings causing strong floods. Composite MSG image contains HRV channel in combination with IR brightness temperatures. Image shows well developed storm tops with cold "U" shape. Land surface was hidden mainly in location signed by cross in red. Storm top is shifted to the north-east by upper air flow but also by parallax effect, which is significant due to high satellite zenith angle.

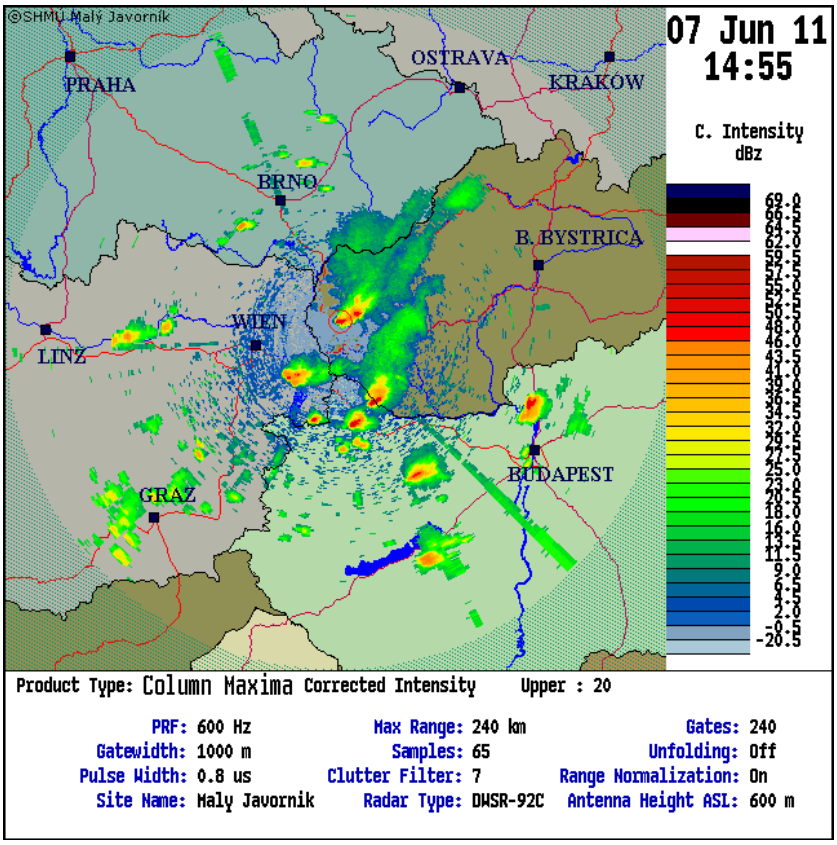

Fig. 6. The storm (shown in Fig. 5) measured by weather radar Malý Javorník. First rain was detected by radar at 11:25 UTC and the same area (signed by red circle) was permanently hided by heavy rains until 15:50 UTC. Total accumulated rainfall exceeded 100 mm.

SHMÚ participates in EUMETSAT DAWBEE project. This initiative was established to promote operational access to EUMETSAT data and products in WMO RA-VI countries, which are not EUMETSAT member states. EUMETSAT procured reception stations and asked experts from Slovakia, Slovenia, Ukraine, Romania, Bulgaria and Croatia to join this project. Installation of the EUMETCast stations in targeted national meteorological services and providing the training for users was the main role of the experts. In addition SHMÚ provided in-house processing and visualisation software which was installed on stations and users were trained to use this software. The project was a good opportunity for SHMÚ to improve the in-house software adding new functionalities – processing of EUMTSAT MPEF (Meteorological Product Extraction Facility) products, generalization for use in different regions and integration into different weather forecasting practices.

References Remote Sensing and Space Meteorology:
(3, 5 and 10 in Slovak)

1. BARKA, I. - BUCHA, T. (2010). Satellite-based regional system for observation of forest response to global environmental changes. In: Horák, J., Halounová, L., Hlásny, T., Kusendová, D., Voženílek, V., eds. Advances in Geoinformation Technologies 2010. Technical University Ostrava, pp. 1–14.

2. BARKA, I. - BUCHA, T. - SITKOVÁ, Z. - HLÁSNY, T. - KULLA, L. (2010). Remote Sensing view on declining spruce forests – Hynutie smrekových porastov očami satelitov. s. 33–47. In: Hlásny T., Sitková, Z., eds. Spruce forest decline in the Beskids – Hynutie smrekových porastov v Beskydoch. NLC Zvolen, 181 pp.

3. BUCHA, T. - VLADOVIČ, J. (2011). Koncept hierarchickej typizácie porastových textúr z údajov DPZ. s. 29–42. In: Vladovič, J., ed. Štruktúra a diverzita lesných ekosystémov na Slovensku. NLC Zvolen, 252 pp.

4. FERANEC, J. - OŤAHEĽ, J. - NOVÁČEK, J. (2010). Slovakia's land cover in 2006 and its change in 2000-2006. In: Bičík I., Himiyama Y., Feranec J., eds. Land use/cover changes in selected regions in the world, 5. IGU-LUCC, Charles University in Prague, Faculty of Sciences, Prague, pp. 17-23.

5. FERANEC, J. - BUCHA, T. - CSAPLÁR, J. - HEFTY, J. - JURAŠEK, M. - KAŇÁK, J. - KUDELA, K. - MACHKOVÁ, N. - SVIČEK, M. - VOJTKO, R. - SCHOLTZ, P. - NOVÁKOVÁ, M. - SZÖCSOVÁ, I. - RAŠI, R. - VLADOVIČ, J. - REICHWALDER, P. - ZEMAN, M. - FINĎO, S. (2010). Slovensko očami satelitov (Satellite's eye view of Slovakia). Veda, Bratislava, 263 pp.

6. FERANEC, J. - SOLÍN, Ľ. - KOPECKÁ, M. - OŤAHEĽ, J. - SOUKUP, T. - BRODSKÝ, L. - KUPKOVÁ, L. - BIČÍK, I. - KOLÁŘ, J. - ŠTYCH, P. (2011). Comparison of selected land cover nomenclatures and their interoperability. In: Halounová L., ed. Remote Sensing and Geoinformation not only for Scientific Cooperation. EARSeL and Czech Technical University, Prague, pp. 352-360. <http://www.earsel.org/symposia//2011-symposium-Prague/Proceedings/index.htm>

7. FERANEC, J. - SOUKUP, T. (2011). Artificial surfaces in Europe: map of changes in 1990-2006. In: 25th International Cartographic Conference 2011 (electronic source). ICA, Paris, 2 pp.

8. GERARD, F. - PETIT, S. - SMITH, G. - THOMSON, A. - BROWN, N. - WADSWORTH, R. - BUGÁR, G. - HALADA, Ľ. - BEZÁK, P. - BOLTIŽIAR, M. - DE BADTS, E. - HALABUK, A. - MOJSES, M. - PETROVIČ, F. - GREGOR, M. - HAZEU, G. - MÜCHER, C. A. -WACHOWICZ, M. - HUITU, H. - TUOMINEN, S. - KÖHLER, R. - OSCHOWSKY, K. - ZIESE, H. - KOLÁŘ, J. - ŠUSTERA, J. - LUQUE, S. - PINO, J. - PONS, X. - RODA, F. - ROSCHER, M. - FERANEC, J. (2010). Land cover change in Europe between 1950 and 2000 determined employing aerial photography. Progress in Physical Geography, 34, 2, 183-205.

9. HAMLÍKOVÁ, Ľ. - KOVÁČIKOVÁ, I. - SVIČEK, M. (2010). The 2010 campaign of remote-sensing control of area-based subsidies. Final report, SSCRI Bratislava, 17 pp.

10. HLÁSNY, T. - BUCHA, T. - KONÔPKA, M. - KOREŇ, M. - BARKA, I. (2011). Hodnotenie vplyvu sucha na porasty duba cerového s využitím satelitných záznamov MODIS, s. 233–238 In: Střelcová, K., Sitková, Z., Kurjak, D., Kmeť, J., eds. Stres suchom a lesné porasty. Technická univerzita vo Zvolene, Národné lesnícke centrum, Ústav ekológie lesa SAV vo Zvolene. 265 pp.

11. KAŇÁK, J. - GEORGIEV, CH. - KRYVOBOK, O. - JERMAN, J. - LIPOVSCAK, B. - DIAMANDI, A. (2011). New possibilities for access and utilisation of EUMETSAT data and products through DAWBEE programme. 2011 EUMETSAT Meteorological Satellite Conference, 5-9 September 2011, Oslo, Norway.

12. NOVÁKOVÁ, M. - KLIKUŠOVSKÁ, Z. - SKALSKÝ, R. - SVIČEK, M. - MIŠKOVÁ, M. - ČIČOVÁ, T. (2010). National system for crop yield and crop production forecasting (in Slovak), SSCRI Bratislava, 32 pp.

13. NOVÁKOVÁ, M. - MIŠKOVÁ, M. – ČIČOVÁ, T. - SVIČEK, M. (2010). Application and actualization of national system of crop yield and crop production forecasting (SK_CGMS) (in Slovak). Final report, SSCRI Bratislava, 41 pp.

14. NOVÁKOVÁ, M. - MIŠKOVÁ, M. - ČIČOVÁ, T. - SVIČEK, M. (2011) Application and actualization of national system of crop yield and crop production forecasting (SK_CGMS) (in Slovak). Final report. SSCRI Bratislava, 50 pp.

15. RINOLLO, A. - PUCA, S. - CAMPIONE, E. - KAŇÁK, J. - KRAHE, P. - RACHIMOW, C. - LÁBÓ, E. - LAPETA, B. - OKON, Ľ. - OZTOPAL, A. - ROULIN, E. - SONMEZ, I. - VULPIANI, G. - PORCU, F. - TORRISI, L. - PAGLIARA, P. - KOYINAROVA, G. - KOSHINCHANOV, G. (2011). A common validation protocol across different countries for the H-SAF precipitation products: ground data quality evaluation and unification of satellite-ground data comparison procedures. 13th Plinius Conference on Mediterranean Storms, 7-9 September 2011, Savona, Italy.

16. SIMON, A. - KAŇÁK, J. - SOKOL, A. - PUTSAI, M. - UHRÍNOVÁ, L. - CSIRMAZ, K. - OKON, Ľ. - HABROVSKÝ, R. (2011). Case study of a severe windstorm over Slovakia and Hungary on 25 June 2008. Atmospheric Research, 100, 705–739.

17. SVIČEK, M. - KOVÁČIKOVÁ, I. (2011). The 2011 campaign of remote-sensing control of area-based subsidies. Final report, SSCRI Bratislava, 20 pp.

6. Institutions involved in Space Research relevant to COSPAR.

Members of the National Committee of COSPAR with e-mail addresses. The website of NC is *http://nccospar.saske.sk*.

Astronomical Institute (AI)
Slovak Academy of Sciences (SAS)
Stará Lesná
059 60 Tatranská Lomnica
J. Rybák (choc@astro.ta3.sk, NC member)

Faculty of Mathematics, Physics and Informatics (FMPI)
Comenius University
Mlynská dolina
842 15 Bratislava
J. Masarik (Jozef.Masarik@fmph.uniba.sk, NC member)

National Forest Centre
T.G. Masaryka 22
960 92 Zvolen
contact: T. Bucha (bucha@nlcsk.org)

Geophysical Institute (GI)
Slovak Academy of Sciences (SAS)
Dúbravská cesta
842 28 Bratislava
M. Revallo (milos.revallo@savba.sk, Secretary of NC)

Institute of Animal Biochemistry and Genetics
Slovak Academy of Sciences (SAS)
Moyzesova 61
900 28 Ivanka pri Dunaji
I. Hapala (Ivan.Hapala@savba.sk, NC member)

Institute of Experimental Endocrinology (IEE)
Slovak Academy of Sciences (SAS)
Vlárska 3
833 06 Bratislava
R. Kvetňanský (ueenkvet@savba.sk, Vice- chair of NC)

Institute of Experimental Physics (IEP)
Slovak Academy of Sciences (SAS)
Watsonova 47
040 01 Košice
K. Kudela (kkudela@kosice.upjs.sk, Chair of NC, Representative of Slovak NC to COSPAR)

Institute of Geography (IGG)
Slovak Academy of Sciences (SAS)
Štefánikova 49
814 73 Bratislava
J. Feranec (feranec@savba.sk, NC member)

Institute of Materials and Machine Mechanics
Slovak Academy of Sciences (SAS)
Račianska 75
831 02 Bratislava 3
J. Lapin (ummslapi@savba.sk, lapin@up.upsav.sk, NC member)

Institute of Measurement Science (IMS)
Slovak Academy of Sciences (SAS)
Dúbravská 9
842 19 Bratislava
contact: I. Frollo (frollo@savba.sk)

Institute of Normal and Pathological Physiology (INPP)
Slovak Academy of Sciences (SAS)
Sienkiewiczova 1
813 71 Bratislava
contact: F. Hlavačka (Frantisek.Hlavacka@savba.sk)

Slovak Environmental Agency
Remote Sensing Department
Tajovského 28
975 90 Banská Bystrica
contact: N. Machková (machkova@sazp.sk)

Slovak Hydrometeorological Institute
Maly Javornik Observatory
827 13 Bratislava
D. Kotláriková (dagmar.kotlarikova@shm.sk, NC member)

Soil Science and Conservation Research Institute
Gagarinova 10
827 13 Bratislava
contact: M. Sviček (svicek@vupu.sk)

Space Research in Slovakia 2010 – 2011
National Committee of COSPAR in Slovak Republic
Slovak Academy of Sciences
Institute of Experimental Physics, SAS, Košice

Editors: Karel Kudela and Ján Feranec

Printed by CopyCenter Košice, March 2012
ISBN 978-80-970779-5-2